

# **Spring-neap tidal cycles modulate the strength of the carbon source at the estuary-coast interface**

Vlad A. Macovei<sup>1</sup>, Louise C.V. Rewrie<sup>1</sup>, Rüdiger Röttgers<sup>2</sup>, Yoana G. Voynova<sup>1</sup>

5 <sup>1</sup>Helmholtz Zentrum Hereon, Institute of Carbon Cycles, Department of Coastal Productivity; Max-Planck-Str. 1, Geesthacht 21502, Germany

<sup>2</sup>Helmholtz Zentrum Hereon, Institute of Carbon Cycles, Department of Optical Oceanography; Max-Planck-Str. 1, Geesthacht 21502, Germany

*Correspondence to:* Vlad A. Macovei (vlad.macovei@hereon.de)

10 **Abstract.** Estuaries are dynamic environments with large biogeochemical variability modulated by tides, linking land to the coastal ocean. The carbon cycle at the land-sea interface can be better constrained by increasing the frequency of observations and by identifying the influence of tides with respect to the spring-neap variability. Here we use FerryBox measurements from a Ship-of-Opportunity travelling between two large temperate estuaries in the North Sea and find that the spring-neap tidal cycle drives a large percentage of the biogeochemical variability, in particular in inorganic and organic  
15 carbon concentrations at the land-sea interface in the outer estuaries and the adjacent coastal region. Of particular importance to carbon budgeting is the up to 74% increase (up to  $43.0 \pm 17.1 \text{ mmol C m}^{-2} \text{ day}^{-1}$ ) in the strength of the estuarine carbon source to the atmosphere estimated during spring tide in a macrotidal estuary. We describe the biogeochemical processes occurring during both spring and neap tidal stages, their net effect on the partial pressure of carbon dioxide in seawater, and the ratios and fluxes of dissolved inorganic and dissolved organic carbon. Surprisingly, while the two example outer  
20 estuaries in this study differ in the timing of the variability, the metabolic state progression and the observed phytoplankton species distribution, an increase in the strength of the potential carbon source to the atmosphere occurs at both outer estuaries on roughly 14-day cycles, suggesting that this is an underlying characteristic essential for the correct estimation of carbon budgets in tidally-driven estuaries and the nearby coastal regions. Understanding the functioning of estuarine systems and quantifying their effect on coastal seas should improve our current biogeochemical models and therefore future carbon  
25 exchange and budget predictability.

**Short Summary.** We found that biogeochemical variability at the land-sea interface in two major temperate estuaries is modulated by the 14-day spring-neap tidal cycle, with large effects on dissolved inorganic and organic carbon concentrations and distribution. Since this effect increases the strength of the carbon source to the atmosphere by up to 74% during spring  
30 tide, it should be accounted for in regional models, which aim to resolve processing at the land-sea interface.

## 1 Introduction

Coastal seas and estuaries are heterogeneous environments characterized by dynamic biogeochemical variability (Bauer et al., 2013), largely driven by river inputs of water, dissolved and suspended matter from land to the coastal ocean (Burson et al., 2016; Frigstad et al., 2020). Estuaries of large rivers undergo biogeochemical variability on regular short-term (day/night  
35 biological cycles and diurnal/semi-diurnal tidal cycles) or medium-term scales (synodic month tidal cycles), as well as irregular variability through flood or drought events affecting the flow rate (Regnier et al., 2013; Joesoef et al., 2017; Shen et al., 2019). They are also affected by anthropogenic activities, which can alter ecosystem functioning, carbon and nutrient cycling, and it can take decades for ecosystems to recover (Rewrie et al., 2023b). Thus, while the variability of estuaries and  
40 coastal oceans can be difficult to capture, it is essential to attempt to quantify the key processes driving this variability at the

land-ocean interface, including how regional physics can affect biogeochemistry (Gattuso et al., 1998; Canuel and Hardison, 2016).

Carbon cycling at the land-sea interface (LSI) still has large knowledge gaps (Legge et al., 2020), since biogeochemical processes, such as primary production, remineralization, carbonate precipitation and dissolution, air-sea and sediment-water exchanges, can all alter the carbonate system over short spatial scales (Cai et al., 2021), and tides can add a further layer of complexity. Generally, estuarine waters are a source of CO<sub>2</sub> to the atmosphere (Borges, 2005; Chen and Borges, 2009; Canuel and Hardison, 2016; Riemann et al., 2016; Volta et al., 2016; Hudon et al., 2017), with a global estimate of 0.25 Pg C yr<sup>-1</sup> (Cai, 2010). In fact, the amount of carbon released to the atmosphere by estuaries could potentially counteract the carbon absorbed by continental shelves (Laruelle et al., 2010). Spring-neap tidal variability can be an important factor influencing carbon biogeochemistry. Previous studies either address this indirectly by focusing on regenerated nutrients (Webb and D'Elia, 1980), light and nutrient availability (Cadier et al., 2017), or by investigating the relationship to chlorophyll dynamics (Xing et al., 2021) and primary production at shelf edges (Sharples et al., 2007; Lucas et al., 2011), or particle settling in the abyssal sea floor (Turnewitsch et al., 2017). Here we investigate the influence of spring-neap variability on the estuary-shelf sea interface, and specifically how it modulates the lateral and vertical carbon fluxes.

With a good understanding of the underlying processes that govern the variability at the LSI, the carbon biogeochemistry in outer estuaries can be modeled and used to better balance the carbon budgets of shelf seas (Ward et al., 2017; Dai et al., 2022). For example, excluding the effect of estuarine plumes from a computation of the annual CO<sub>2</sub> flux in the southern North Sea increased the sea-to-air flux by 20% (Schiettecatte et al., 2007). Challenges remain – for example, a coupled hydrodynamic-ecosystem model used to investigate the impact of coastal acidification in the North Sea was still not able to reproduce *p*CO<sub>2</sub> correctly (Artioli et al., 2012). Numerous studies found that the best way to capture and assess the intrinsic estuarine heterogeneity and tidal complexity is to increase observations, so as to correctly identify and characterize the processes in regions where observations already exist (Schiettecatte et al., 2007; Kuliński et al., 2011; Voynova et al., 2015; Regnier et al., 2022). In an estuarine setting for example, high-frequency observations are particularly important due to the large horizontal gradients present (Kerimoglu et al., 2018; Cai et al., 2021). Furthermore, the difference in the tidal energy between spring and neap tides influences the location and intensity of mixing processes (Chegini et al., 2020). A high observational frequency that is able to capture both space and time variability can be achieved with Ship-of-Opportunity (SOO) measurements (Jiang et al., 2019).

In a recent study, Macovei et al. (2022) observed high seawater *p*CO<sub>2</sub> outside the Humber River estuary, as well as variability that seemed to match the spring-neap tidal cycles. However, the authors found that while the Copernicus Marine Environment Biogeochemical Shelf Sea Model (Butenschön et al., 2016) captured the *p*CO<sub>2</sub> spatial distribution in the central North Sea, in the nearshore, outer estuary region, neither the overall *p*CO<sub>2</sub> levels, nor the variability in *p*CO<sub>2</sub> were accurately

75 reproduced. Furthermore, not accounting for the influence of estuaries in coastal regional models, as evidenced by Canuel  
and Hardison (2016), raises the uncertainty of carbon budget estimations, and can lead to erroneous results. A recent study  
showed that rivers perturb the coastal carbon cycle to a larger extent offshore than previously considered (Lacroix et al.,  
2021), and can influence coastal regions with changes in estuarine discharge (Garvine and Whitney, 2006; Voynova et al.,  
2017; Kerimoglu et al., 2020). In addition, the land-based inputs and the partitioning between the inorganic and organic  
80 carbon forms is needed for regional budget calculations (Kitidis et al., 2019). In this context, this study examines the tidally-  
driven spring-neap biogeochemical variability in the outer estuaries of two large European rivers, characterizes this  
variability with respect to the carbon concentrations and fluxes at the LSI and quantifies the largely unaccounted impact on  
regional carbon budget assessments.

## 2 Methods

### 85 2.1 Study area

The North Sea as a whole has been previously characterized as an important carbon sink (Thomas et al., 2005), but recently,  
driven by summertime biological activity, a decrease in the buffer capacity and a diminishing efficiency of the continental  
shelf pump (Tsunogai et al., 1999), its carbon uptake capacity has weakened (Lorkowski et al., 2012; Clargo et al.,  
2015; Bourgeois et al., 2016). The seawater  $p\text{CO}_2$  in the North Sea was found to increase at a faster rate than the atmospheric  
90 one, mainly driven by non-thermal effects in the summer months, shifting the carbon uptake/release boundary northwards  
(Macovei et al., 2021a). This affects the Central North Sea, which separates the northern region as a dominant sink from the  
southern region as an overall source of  $\text{CO}_2$  to the atmosphere. This creates a fragile balance regarding the direction of the  
carbon dioxide flux, which depends on the dominance of thermal or biological forcing (Hartman et al., 2019; Kitidis et al.,  
2019). The North Sea is therefore an ideal location to investigate this variability at the LSI using long-term and high-  
95 frequency observations. The MS *Hafnia Seaways* (DFDS Seaways, Copenhagen, Denmark) is a cargo vessel that regularly  
transited the North Sea between 2014 and 2018. The ship was equipped with a FerryBox as part of the Coastal Observing  
System for Northern and Arctic Seas - COSYNA (Baschek et al., 2017) and travelled between Immingham, UK and  
Cuxhaven, Germany. These ports are located within the outer estuaries of the Humber and Elbe Rivers respectively, two  
tidally-driven estuaries with different characteristics and catchment regions (Fig. 1). While the carbon dynamics in the  
100 Central North Sea have been previously assessed (Macovei et al., 2021a), this work is focused on the land-sea interface, and  
in particular the two temperate estuaries and their adjacent coastal regions specified in Fig. 1c and 1d.

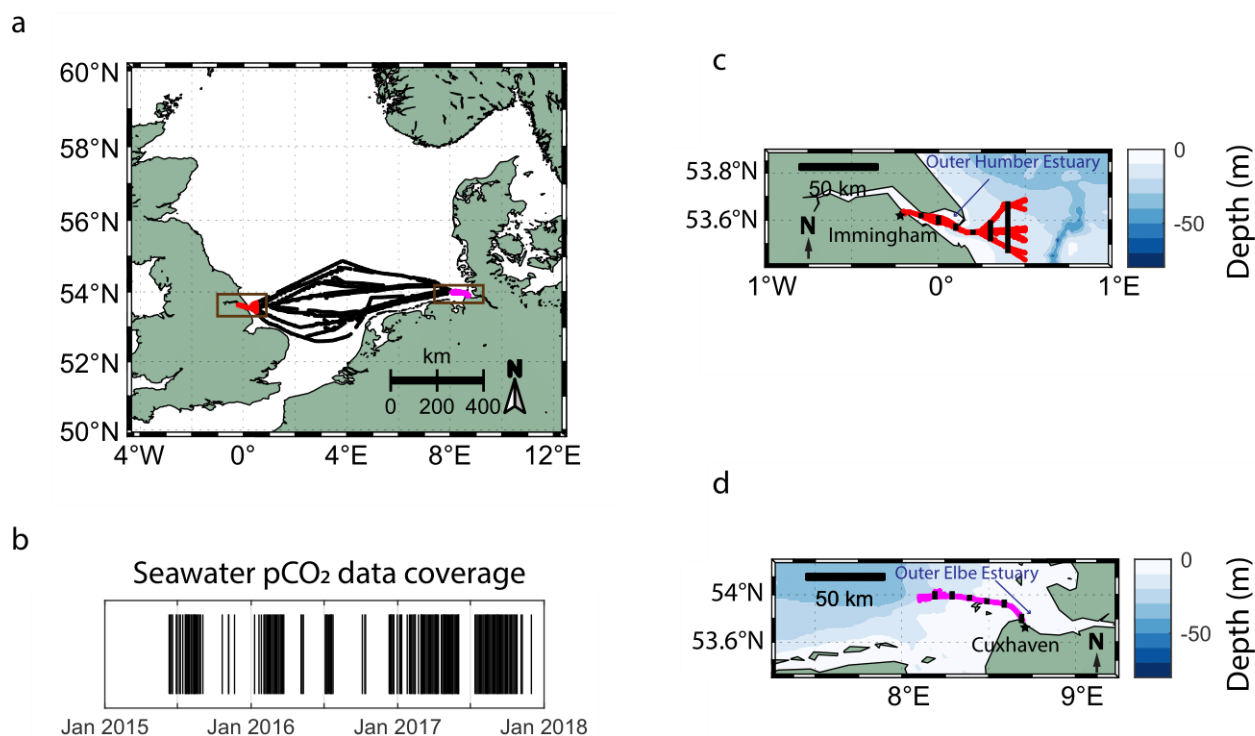


**Figure 1:** The SOO routes (a) and the temporal  $p\text{CO}_2$  data coverage (b) of MS *Hafnia Seaways* travelling in the North Sea between 2015 and end of 2017. Black markers in panel b indicate the available measurements during this period. A zoom-in on the locations of the near-shore measurements (brown boxes in panel a) used in this study (red and magenta) and the NOAA ETOPO2 bathymetry near Immingham, UK (c) and Cuxhaven, Germany (d) are also shown. In panels c and d, the location of the selected samples for the box plot analysis in Figures 3 and 5 is indicated by black markers.

The Humber River catchment extends over 24,000 km<sup>2</sup> and its average river discharge (1990-1993) is England's largest at 250 m<sup>3</sup> s<sup>-1</sup> (Sanders et al., 1997). Its geology is Carboniferous limestone in the west and Permian and Triassic sandstone in the east, while the overlying Quaternary deposits are mostly clays (Jarvie et al., 1997b). The catchment area is a mix of industrialized, agricultural and urban areas, and the anthropogenically-influenced runoff affects the biogeochemical processes in the estuary (Jarvie et al., 1997a). Between 70 and 80% of the catchment is arable land or grassland, and the agricultural practices cause the nitrate concentrations in the surface waters to frequently exceed the 50 mg L<sup>-1</sup> EU Nitrates Directive standard (Cave et al., 2003). The excess nutrients are carried to the estuary, which starts at Trent Falls, about 60 km inland from the coast, but estuarine primary production is strongly light-limited by high turbidity (Jickells et al., 2000). Therefore, most nutrients are likely transported offshore, rather than assimilated in the estuary. The estuary outflows of the Humber and other British east coast rivers form the East Anglian plume, which influences primary production in the Southern North Sea further offshore of the immediate river and estuary outflows, reaching as far as the Southern Bight of the

North Sea (Dyer and Moffat, 1998; Weston et al., 2004). The effluent from industrial sources increases the biological oxygen demand in the estuary, and therefore the Humber estuary oxygen concentrations are low (Cave et al., 2003). Tides in the Humber estuary are semi-diurnal and the tidal range of up to 7.2 m makes it a macro-tidal and well-mixed estuary.

125 The Elbe River catchment extends over 148,000 km<sup>2</sup>, with an average river discharge (2005-2007) of 730 m<sup>3</sup> s<sup>-1</sup>, making it one of Europe's largest rivers (Schlarbaum et al., 2010). The source of the river is found in Czechia in the Giant Mountains, primarily made of granite. The Elbe then flows through sandstone mountains before crossing the flat fertile marshlands of north Germany. River water chemistry is strongly correlated with the watershed geology (Newton et al., 1987), so one would expect the alkalinity in the Elbe to be lower than in the Humber River, which flows through limestone bedrock. However, 130 Hartmann (2009) found that the carbonate abundance in silicate-dominated geology is also important. In addition, erosion rate, mean annual temperature, catchment area and soil regolith thickness, all can influence the river carbon chemistry (Lehmann et al., 2023). The anthropogenic pressure in the Elbe watershed is high, with most of the catchment being dominated by agricultural land use (Quiel et al., 2011). While water quality has improved since the 1980s (Dähnke et al., 2008; Amann et al., 2012; Rewrie et al., 2023b), the measures have disproportionately reduced the phosphorus input, so the 135 current nutrient load has an increased nitrogen to phosphorus ratio (Geerts et al., 2013). The Elbe Estuary extends from the Geesthacht Weir to the mouth of the estuary at Cuxhaven, Germany, a further 141 km downstream. The large port of Hamburg, situated in the upper estuary, also increases the anthropogenic pressure in the estuary due to regular dredging and industrial activities that facilitate the development of oxygen depleted zones (Geerts et al., 2017). Tides are semi-diurnal, and with a tidal range of up to 4 m. Therefore, the Elbe Estuary falls between a meso- and macro-tidal estuary and the salinity 140 profiles classify it as a partially-mixed to well-mixed estuary (Kerner, 2007).

## 2.2 FerryBox measurements

FerryBoxes are modular automated measurement systems that can be installed on SOOs or fixed stations to provide high-frequency observations of sea surface waters (Petersen, 2014). Their characteristics make them ideal as autonomous 145 biogeochemical observatories on moving platforms (Petersen and Colijn, 2017). FerryBoxes are mature platforms with a well-established FerryBox community and EuroGOOS FerryBox Task Team. Many publications have used FerryBox data in our study area (Voynova et al., 2019; Kerimoglu et al., 2020; Macovei et al., 2021a) and Chegini et al. (2020), for example, use FerryBox measurements to identify and characterize the effect of spring and neap tides to the stratification regime in the German Bight. A suite of instruments were installed on the MS *Hafnia Seaways* (Table 1). Quality controlled temperature, 150 salinity and *p*CO<sub>2</sub> data obtained by this SOO are now publicly available on the Pangaea repository (<https://doi.org/10.1594/PANGAEA.930383>) and have been used in a previous study evaluating surface seawater *p*CO<sub>2</sub> trends (Macovei et al., 2021a). All other data are currently available in the European FerryBox Database (<https://ferrydata.hereon.de>) and on the COSYNA data portal (Baschek et al., 2017).

155 **Table 1:** FerryBox-integrated instruments installed on MS *Hafnia Seaways*, measuring between 2015 and 2017 and used in this study.

Parameter	Instrument	Manufacturer	Uncertainty
Seawater temperature and salinity	Citadel TS-N	Teledyne Technologies/Falmouth	$\pm 0.1\text{ }^{\circ}\text{C}$ and $\pm 0.02$ , respectively
	Thermosalinograph	Scientific, United States	
Seawater $p\text{CO}_2$	HydroC $\text{CO}_2$ -FT membrane-	CONTROS Sensors, 4H-Jena	$\pm 1\%$
	based equilibration sensor	Engineering GmbH, Germany	
Seawater pH (total scale)	Ion Selective Field Effect	Endress+Hauser GmbH, Germany	$\pm 2\%$
	Transistor (ISFET)		
Total chlorophyll- <i>a</i> fluorescence- derived concentration and plankton species distribution	AlgaeOnlineAnalyser	bbe Moldaenke GmbH, Germany	$0.01\text{ }\mu\text{g L}^{-1}$
	(AOA)		
Total chlorophyll- <i>a</i> fluorescence- derived concentration	ECO FLNTU Fluorometer	WET Labs, Sea-Bird Scientific, United States	$0.025\text{ }\mu\text{g L}^{-1}$
	and scattering meter		
Turbidity	Turbimax W CUS31	Endress Hauser GmbH, Germany	$< 5\%$
	Turbidity sensor		
Chromophoric Dissolved Organic Matter (CDOM) fluorescence- derived concentration	microFlu Fluorometer	TriOS Mess- und Datentechnik GmbH,	$\pm 5\%$
		Germany	
Dissolved Oxygen	4330F Optode	Aanderaa Instruments,	$\pm 2\text{ }\mu\text{M}$ or $\pm 1.5\%$
		Xylem Analytics, Germany	

During the data collection period (2.5 years), 53 maintenance visits were performed. The flow cells of the sensors were cleaned and, if deemed necessary, the sensors were replaced. New sensors are always calibrated by the manufacturer, with documentation provided. The temperature and salinity sensor, the WET Labs chlorophyll sensor and the CDOM sensor were not changed. The  $p\text{CO}_2$  sensor was changed 4 times and appropriate data processing methods were applied, as described by Macovei et al. (2021b), to ensure a span-drift correction, and quality-controlled (Macovei et al., 2021c) to ensure no abrupt

changes in the data occurred. The ISFET pH sensor was changed once, the AOA chlorophyll sensor was changed 3 times, the oxygen optode was changed 3 times, with verification samples collected 22 times.

165 The FerryBox system starts measurements automatically based on the GPS location after departure from port. Since some instruments need time to reach optimal functioning, we only use data from the ship's journeys arriving to port. The arrival time into ports was consistent, irrespective of the tidal stage or sea level (Fig. 2a,b). Since high and low tides progress every day (12.5 hour cycle), a long time series, like those used in this study, likely will include all tidal stages with no bias. All the statistical analyses are made using original, quality-controlled data. There are sufficient data without gaps to capture  
170 consecutive spring and neap tide events and also to characterize the typical state of the system during the spring and neap tidal stages.

### 2.3 Processing of FerryBox data

The turbidity sensor was calibrated using discrete samples collected by the auto-sampler installed on board the vessel and  
175 measured in the laboratory between February 2016 and July 2017 ( $R^2=0.92$ ,  $n=19$ ). Measurements at the upper limit of detection or above were discarded.

The FerryBox was equipped with a bbe-Moldaenke algal online analyser (AOA), which provided valuable information about the relative distribution of plankton classes contributing to the total pigment signal (Wiltshire et al., 1998). The sensor can  
180 usually differentiate between diatoms, green algae, blue-green algae and cryptophytes. However, the total chlorophyll was likely overestimated by this instrument. We also measured total chlorophyll with a WET Labs sensor. We compared the WET Labs measurements with laboratory high-performance liquid chromatography (HPLC) measurements, collected in March 2016 from the onboard autosampler ( $R^2=0.94$ ,  $n=4$ ). The AOA measurements were then calibrated to the corrected WET Labs measurements. Since during the study period, four different AOA instruments were used, linear relationships  
185 were calculated for each instrument deployment in each of the two outer estuaries, with coefficients of determination ranging from 0.52 to 0.95 (details in Fig. S1).

Between February 2016 and November 2017, the performance of the ISFET pH sensor was evaluated eleven times during maintenance visits by measuring buffer solutions with pH values of 7.0 and 9.0. Using the time regression of the difference  
190 between the measurements and the standards, we assessed that the instrument exhibited a drift of 0.00045 pH units per day, which we corrected for before reporting the final results.

We used the Matlab CO2SYS toolbox (van Heuven et al., 2011) with the Cai and Wang (1998) K1 and K2 dissociation constants, which are appropriate for salinities as low as 0 and the Dickson et al. (1990) K SO<sub>4</sub> constant to calculate dissolved



195 inorganic carbon (DIC) concentrations from  $p\text{CO}_2$  and pH. We converted the ISFET pH measured on the total scale to the NBS scale before calculating, in order to fit the requirements of the dissociation constants used. This conversion was performed using CO2SYS, with the associated values of temperature, salinity and  $p\text{CO}_2$  for each pH value. To compare with the dissolved organic carbon (DOC) concentrations, the DIC concentrations were converted to  $\mu\text{mol L}^{-1}$  using the Gibbs Seawater Toolbox for Matlab (McDougall and Barker, 2011). An empirical relationship between CDOM fluorescence, expressed on the quinine sulfate (QSU) scale and DOC concentration was used to calculate the latter. This relationship was based on the measurements of DOC concentrations and CDOM fluorescence during the research cruise HE407 with RV *Heincke*, which took place in August 2013 in the outer Elbe Estuary and German Bight. Water samples were analyzed in the laboratory and the following linear relationship ( $R^2=0.67$ ,  $n=10$ ) was found with results from the Trios microFlu CDOM fluorometer integrated on the FerryBox on-board:  $\text{DOC} [\mu\text{mol L}^{-1}] = 10.75 \times \text{CDOM} [\mu\text{g L}^{-1}] + 162.06$ . While we acknowledge the limitations of using an empirical relationship based on a single cruise, this relationship is close to other literature references discussed below, and the resulting DOC concentrations fall within the range of direct water sample measurements made by the Flussgebietsgemeinschaft Elbe. Converting the proxy CDOM results into estuarine DOC concentrations is useful for understanding the partitioning of dissolved carbon between the inorganic and organic fractions.

## 210 2.4 Additional data

Sea level data at the Immingham Docks were obtained from the British Oceanographic Data Centre ([https://www.bodc.ac.uk/data/hosted\\_data\\_systems/sea\\_level/uk\\_tide\\_gauge\\_network/processed/](https://www.bodc.ac.uk/data/hosted_data_systems/sea_level/uk_tide_gauge_network/processed/)). Sea level data at the Cuxhaven Pier were obtained from the German Federal Waterways and Shipping Administration (WSV), communicated by the German Federal Institute of Hydrology (BfG) (<https://www.pegelonline.wsv.de/gast/stammdaten?pegelnr=5990020>). The reporting frequency of the datasets were 15 minutes and 1 minute, respectively. In order to extract the spring-neap tidal cycle, sea level data were processed by running a moving maximum and a moving minimum calculation with a 100-hour window, in order to smooth the time series. The highest (lowest) difference between the 100-hour smoothed maximum and minimum sea level occurs during spring (neap) tides, with a recurrence interval approximately matching the literature value of 14.77 days (Kvale, 2006). The times of the spring and neap tides were identified with a peak search function on the smoothed tidal range. Data were categorized by assigning measurements taken within  $\pm 25$  hours of the identified peaks to spring tide or neap tide periods, respectively.

We cross-checked our findings with fixed-point salinity data from the Cuxhaven observing station, equipped with a FerryBox and situated at the outflow of the Elbe Estuary into the North Sea. This station is now also part of the ICOS-D network (since 2023) and has been successfully used by Rewrie et al. (2025) to estimate primary production and net ecosystem metabolism at the LSI. The time span of this dataset is 2020-2022, after a CDOM fluorescence sensor was installed. While this is a few years later than the MS *Hafnia Seaways* dataset, the comparison to a station with a high

temporal resolution is valuable. To the best of our knowledge, there is no equivalent biogeochemical observing station in the Humber Estuary.

230

Atmospheric carbon dioxide measurements were obtained from the Mace Head observatory in Ireland (World Data Centre for Greenhouse Gases, 2020). These are reported as dry air mole fraction ( $x\text{CO}_2$ ), expressed in ppm. We used barometric pressure, dew point temperature and 10 m wind speed from the ERA5 reanalysis product (Hersbach et al., 2018) selected for the closest pixel to the Humber Estuary region, as provided by the Copernicus Climate Data Store (https://cds.climate.copernicus.eu). When estimating sea-to-air carbon fluxes, we calculated average values of the years 2015-2017 for the required input terms. The atmospheric  $x\text{CO}_2$  was converted to  $p\text{CO}_2$  using the saturated water vapor pressure formula from Alduchov and Eskridge (1996).

235

Finally, we used the Drift App of the CoastMap Geoportal (https://hcdc.hereon.de/drift-now/) under CC BY-NC 4.0 license to simulate water mass movement in our study areas. This application specifies drift trajectories using the Lagrangian transport program PELLETS-2D (Callies et al., 2011). Drift simulations are based on two-dimensional marine currents extracted from archived output of the three-dimensional hydrodynamic model BSHcmod that is run operationally at BSH. The tool has successfully been used for particle and water mass tracking applications (Callies, 2021; Callies et al., 2021). We simulated 24-hour backward trajectories from selected locations in the two outer estuaries starting both at the high and low tides during spring and neap tide conditions, which we selected from the sea level data.

240

245

### 3 Results

The frequency of the repeating ship journeys to each port is too low to resolve the semi-diurnal high and low tides that characterize the two estuaries, but it is high enough to provide data during each stage of a spring-neap tidal cycle. Our observations were showing cyclical variability, so we applied spectral analysis on our dataset using the fast Fourier transform method with the Matlab *fft* function. The signal with the highest power had a period of 14.5 days for the Humber estuary and 14.1 days for the Elbe estuary, indicating that spring-neap cycling is the main mode of  $p\text{CO}_2$  variability for SOO data in these regions (Fig. 2c). We applied the same analysis to continuous (1 minute resolution) salinity data from the Cuxhaven observing station with the dominant period at 12.4 hours, indicating that the semi-diurnal tides dominate the variability at the resolution provided by the station. After filtering out the high frequency data with a 3.5-day moving average, the dominant frequency in the power spectral density plot occurred at 14.5 days revealing the spring-neap-driven biogeochemical variability in the station data too (Fig. 2d). Further examples of Cuxhaven station data demonstrate two-weekly variability in biogeochemical parameters such as CDOM (Fig. 2e) and turbidity (Fig 2f). For a similar investigation

250

255

of arrival time and spectral analysis in the outer Humber Estuary and further data from the Cuxhaven station see the  
 260 Supplementary Material Fig. S2).

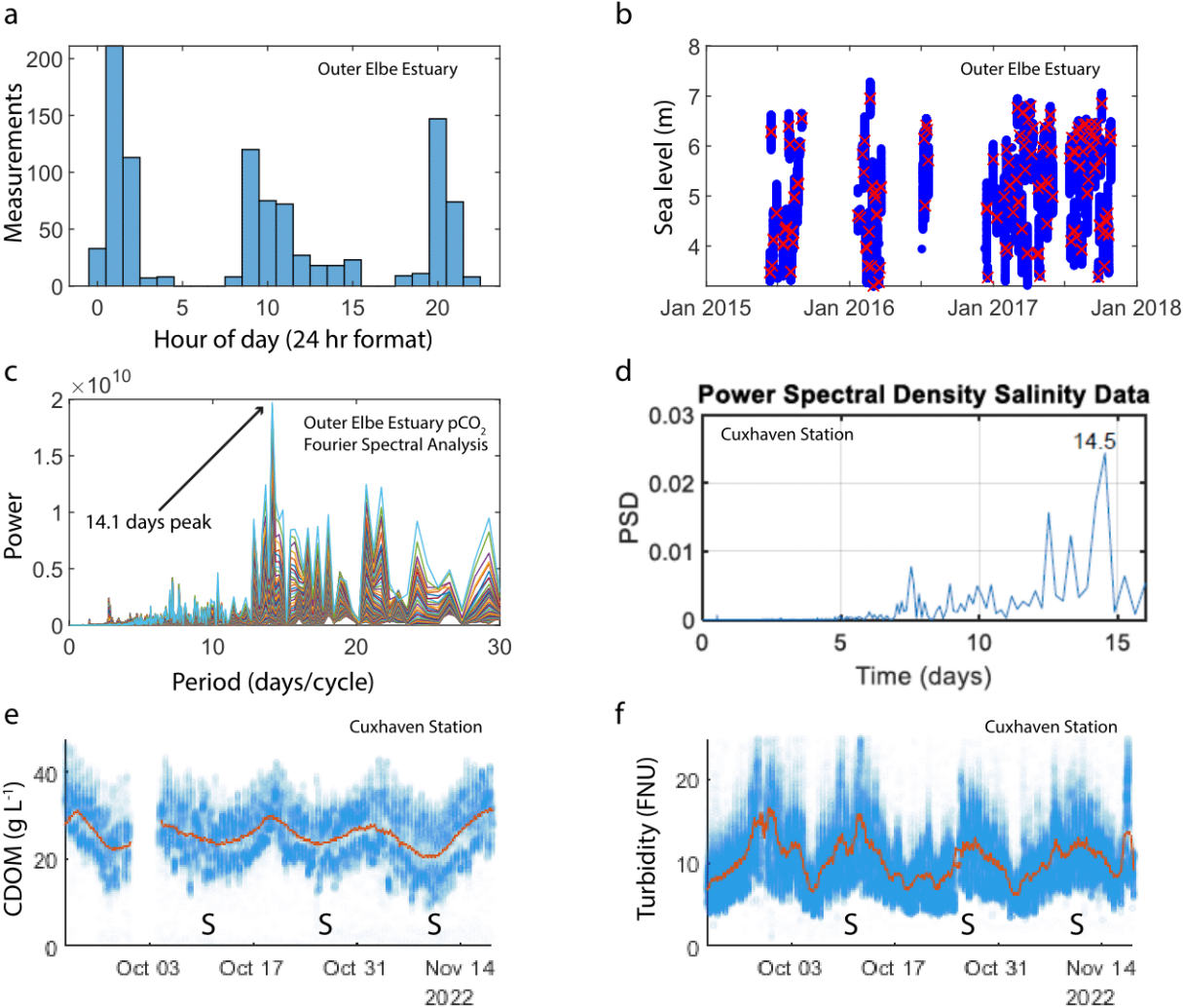


**Figure 2:** (a) Histogram showing the ship arrival time in Cuxhaven port in the outer Elbe Estuary. (b) The sea level at the arrival time (red crosses) compared to the usual sea level range (blue dots) in the outer Elbe Estuary. (c) The power versus period (inverse of frequency) plot resulting from a fast Fourier transform analysis on  $p\text{CO}_2$  SOO data in the outer Elbe Estuary. (d) A Fourier analysis of the salinity data  
 265 from the Cuxhaven fixed-point measurement station in the outer Elbe Estuary performed on a 3.5 day moving average to filter out the high frequencies, which would produce a strong 12.5 hour peak. The resulting power spectral density plot shows a peak at 14.5 days. We are also showing the cyclical biweekly biogeochemical variability at Cuxhaven by selecting observations from a two month period in fall 2022. The CDOM (e), and turbidity (f) observations are shown in blue markers and a 3.5 day moving average is shown in orange. Spring tides are indicated with “S” on the time axes.

### 270 3.1 Tidally-controlled biogeochemistry in the Humber estuary and adjacent coast

The SOO observations reveal that biogeochemical parameters in the outer Humber Estuary vary according to the spring-neap tidal cycle. We selected all available measurements (Fig. 1c) around six positions based on the longitude ( $\pm 0.005^\circ$  around every  $0.1^\circ$ ) and further split and sorted them into times when spring or neap tides are expected (Fig. 3). The chosen locations demonstrate the gradients from port, through the outer estuary and to the adjacent coastal sea waters. For other methods of selecting the data with similar results, see Fig. S3. Statistical differences between groups are assessed using a Welch's t-test (Matlab function `ttest2`), with a rather strict significance level of 0.01 to avoid false positives. This statistical method tests the null hypothesis that two populations, with not-necessarily equal variances, have equal means, and is appropriate to compare our spring and neap tide groups.

280

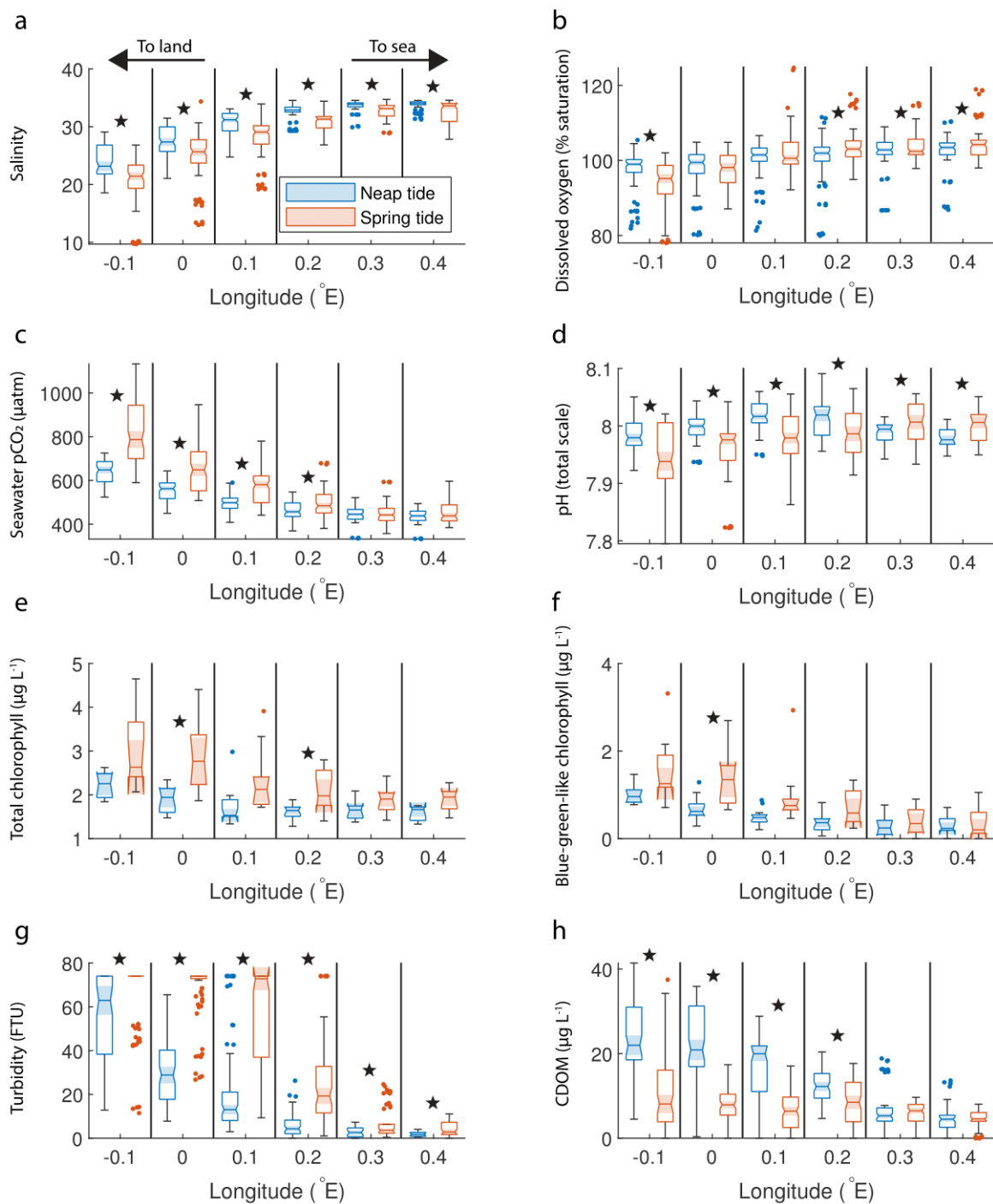


**Figure 3:** Box plots of salinity (a), dissolved oxygen saturation (b), seawater  $pCO_2$  (c), pH (d), total chlorophyll concentration (e), blue-green-like chlorophyll concentration (f), turbidity (g) and CDOM (h) grouped in six regions in the outer Humber Estuary, comparing the

285 neap (blue) and spring (red) tide measurements. The box plots display the median, interquartile range and outliers. When the notches of two box plots do not overlap, they have different medians at the 5% significance level. We are also indicating statistical difference between spring and neap tide measurements with symbols above the specific pair. Spring tide turbidity values are above the upper limit of detection in the westernmost two box plots in subfigure (g), and are therefore reported as this maximum value, without variance. Star symbols indicate statistically significant differences between spring and neap tide groups assessed with Welch's t-test.

290

Significant differences between the mean spring tide and the mean neap tide results indicated that during spring tide, salinity was significantly lower than during neap tide at all locations (Fig. 3a). Both the spring and neap tide selected datasets captured various stages of the semi-diurnal tidal cycle. For example, at the most upstream location the spring tide salinity during low tides was  $18.9 \pm 0.3$  and during high tides  $22.6 \pm 0.7$ , while during neap tides, the salinity was  $22.6 \pm 2.4$  during 295 low tides and  $25.8 \pm 3.2$  during high tides. Stronger oxygen undersaturation was observed during spring tides (Fig. 3b). Seawater  $p\text{CO}_2$  was significantly higher during spring tide at the four westernmost locations in the outer Humber Estuary, with a maximum median value of  $787 \mu\text{atm}$  (interquartile range 700 to  $844 \mu\text{atm}$ ) (Fig. 3c). At the same four locations, spring tide pH was significantly lower than neap tide pH, while surprisingly, spring tide pH was significantly higher than neap tide values at the easternmost offshore locations (Fig. 3d). The total chlorophyll-*a* (Fig. 3e) and blue-green signal 300 from the AOA measurements (Fig. 3f) had high variance, but generally had higher values during spring tides. Turbidity was significantly higher at spring tide than at neap tide at all chosen locations (Fig. 3g). CDOM had a reverse pattern to turbidity and  $p\text{CO}_2$ , with spring tide values significantly lower than neap tide values at the four westernmost locations (Fig. 3h). Most variables show a gradient between the estuary and the offshore regions. Salinity medians ranging from 21 to 31, were lower than the North Sea salinity (32 to 35), and the low salinity plume was observed up to  $0.2^\circ\text{E}$ , or 7 km offshore from the 305 estuary mouth. There was also a west-to-east gradient in the oxygen saturation measurements. Turbidity, total and blue-green-like chlorophyll-*a*, and CDOM were all lower offshore than in the estuary. In fact, during spring tide, turbidity measurements exceeded the upper limit of the sensor ( $\sim 74$  Formazine Turbidity Units, FTU).

The results presented in Fig. 3 show that the outer Humber Estuary experiences two distinct states, depending on the spring- 310 neap tidal cycle. The advantage of the repeating ship journeys is that the transition between these states and the cyclical variability were observed. In order to show this, we chose a two-month period with relatively good data coverage and present the Humber estuary data as a Hovmöller plot (Fig. 4). We show the same variables as in Fig. 3 and we overlay a line plot of the tidal range to collocate the spring and neap tidal cycle with the observed changes in the biogeochemical parameters. This addition helps to show the relationship between the physical forcing and the biogeochemical response.

315

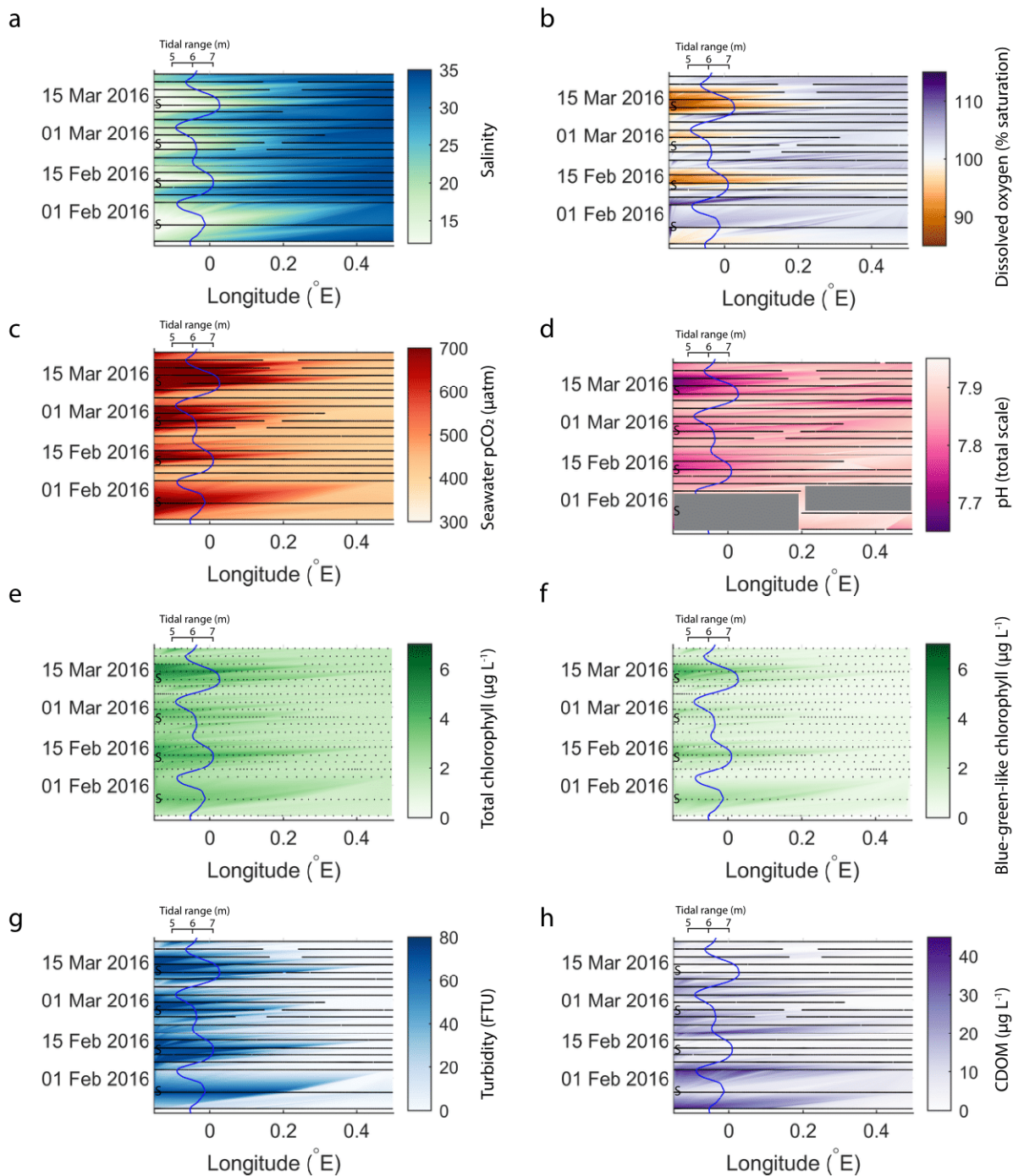


**Figure 4:** An example of fortnightly variability in biogeochemical parameters in the outer Humber Estuary matching the spring-neap tidal cycle. The time/longitude coordinates of the measurements are shown in black. The tidal range is shown with the blue line and spring tides

320 are indicated with “S”. Large data gaps are masked out with gray boxes. The variables shown are salinity (a), dissolved oxygen saturation (b),  $p\text{CO}_2$  (c), pH (d), total chlorophyll (e), blue-green-like chlorophyll (f), turbidity (g) and CDOM (h).

In the two-month period shown in Fig. 4, four spring tides and four neap tides occurred. The transition between the two tidal states was influenced by the tidal range by modulating the strength of the estuarine influence. For example, the offshore  
325 extent of the spring tide-driven conditions, as well as the maximum levels reached during the less-pronounced spring tide event (24 February 2016) were smaller for most variables presented here, except for salinity and  $p\text{CO}_2$ . Similar to the median conditions in 2015-2017 (Fig. 3), CDOM was higher during neap tide. Especially further upstream in the estuary, the physical and biogeochemical variability was large and correlated with the spring-neap tidal cycles. From neap to spring tide, the seawater changed from a salinity of 15, oxygen undersaturation and high carbon dioxide oversaturation to a salinity  
330 higher than 25, oxygen oversaturation and carbon dioxide close to atmospheric balance. In the estuary region, turbidity was below 20 FTU during neap tides and above the detection limit of 74 FTU during spring tides.

### 3.2 Tidally-controlled biogeochemistry in the outer Elbe Estuary

The ship stopped at the mouth of the Elbe Estuary at Cuxhaven (Fig. 1d), but we were able to observe the estuarine signal:  
335 the median of the salinity measurements at the easternmost location was low, at around 19 for both spring and neap tide (Fig. 5a). This region has been described as the outer Elbe Estuary (Rewrie et al., 2023b) and is known to feature rapid changes in  $p\text{CO}_2$  with changing salinity (Brasse et al., 2002). The high interquartile range at this location makes differentiating spring and neap tide measurements more difficult. Salinity increased offshore off the estuary outflow, but unlike in the Humber, statistically significant lower salinity was observed during neap tides. The medians of the oxygen measurements were higher  
340 than 100% saturation, except in the region closest to Cuxhaven, where a significant difference between spring and neap tide oxygen was observed, with neap tide oxygen significantly lower (Fig. 5b). Seawater  $p\text{CO}_2$  was generally higher towards the estuary, and above the atmospheric level with medians ranging from 422 to 594  $\mu\text{atm}$ . Unlike in the Humber, in the outer Elbe Estuary there was no difference between the spring and neap tide in seawater  $p\text{CO}_2$ , except at two locations (8.39 °E and 8.69 °E) where the Welch’s t-test showed that neap tide  $p\text{CO}_2$  values were significantly higher than the spring tide  $p\text{CO}_2$   
345 values (Fig. 5c). Furthermore, in the outer Elbe Estuary, the seawater  $p\text{CO}_2$  values were overall lower than in the Humber Estuary, and closer to atmospheric balance. There was no significant difference in spring-to-neap pH, with little variability, and medians between 8 and 8.05 depending on location (Fig. 5d). Similar to the Humber Estuary, the total and blue-green chlorophyll-*a* concentrations in the Elbe Estuary showed a high variance (Fig. 5e,f). Unlike in the Humber however, there was no statistical difference between spring and neap tide and the blue-green-like chlorophyll-*a* concentrations were not  
350 proportionally as high. Turbidity was generally below 20 FTU except for some outliers (Fig. 5g). Similar to the Humber Estuary, neap tide CDOM measurements (Fig. 5h) were higher than spring tide and the maximum measurements were recorded upstream, at lower salinities. We split the high-resolution fixed-point data from the Cuxhaven station in the same



way as the ship data. There were statistically significant differences (Welch's t-test at the 1% confidence level) between spring and neap tide data for the biogeochemical variables we tested. Furthermore, investigating a two-month period in more  
355 detail clearly displays a two-week spring-neap cycle (Fig. 2e,f).

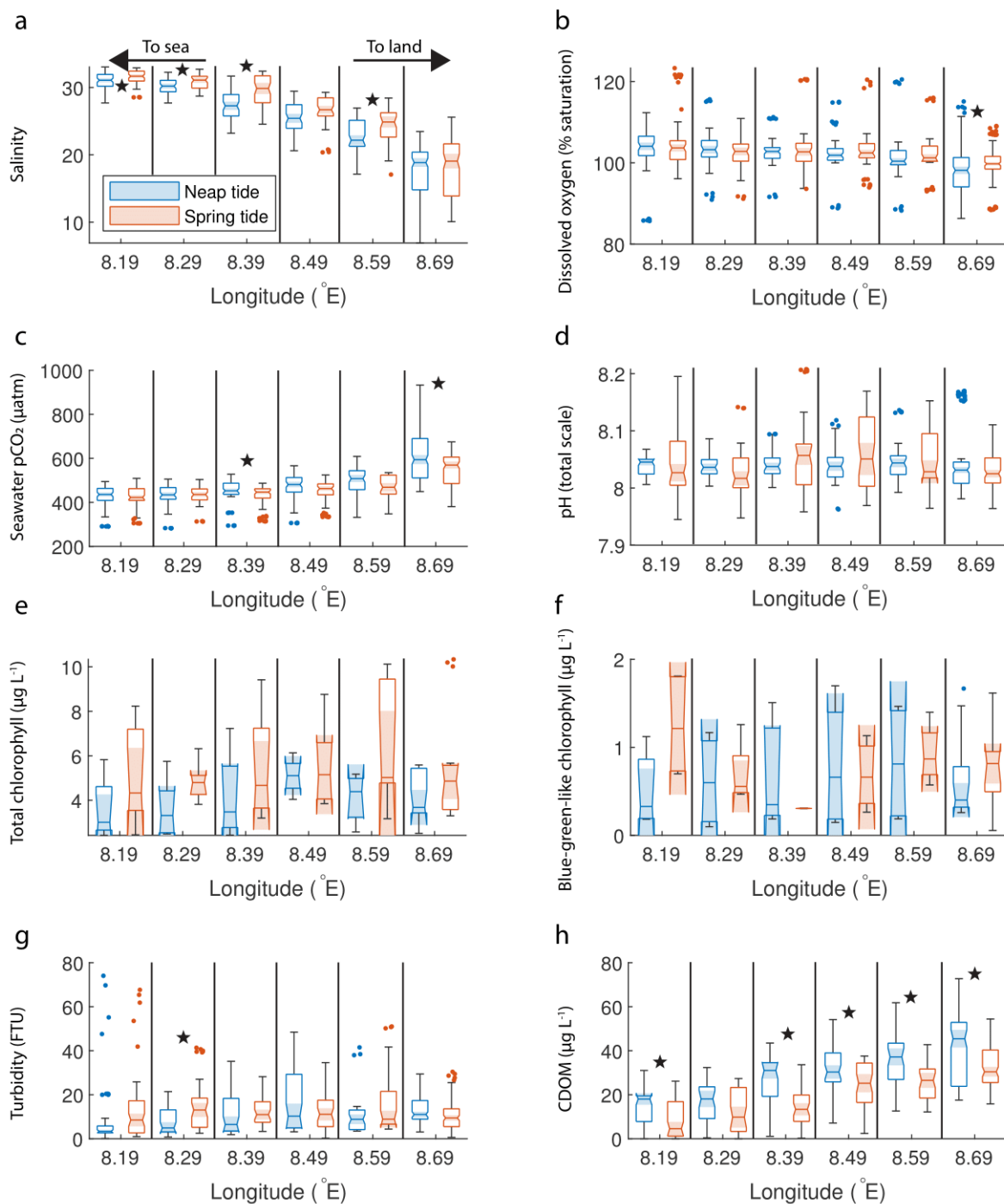


**Figure 5:** Box plots of salinity (a), dissolved oxygen saturation (b), seawater  $p\text{CO}_2$  (c), pH (d), total chlorophyll concentration (e), blue-green-like chlorophyll concentration (f), turbidity (g) and CDOM (h) grouped in six regions in the outer Elbe Estuary, comparing the neap

(blue) and spring (red) tide measurements. The box plots display the median, interquartile range and outliers. When the notches of two box plots do not overlap, they have different medians at the 5% significance level. Welch's t-test statistically significant differences between spring and neap tide groups are indicated with star symbols.

365 Figure 6 presents data from the same period as in Fig. 4, but in the outer Elbe Estuary. The tidal range is again shown on a  
secondary axis, but this time the axis is reversed so that spring tide events are represented by the curve moving away from  
the river end on the right side of the diagram. The tidal range, usually between 3.25 and 4.25 m, was smaller than in the  
Humber Estuary. The typical conditions that coincided with the peak spring tide in the Humber Estuary – low salinity,  
oxygen undersaturation, high  $p\text{CO}_2$ , high chlorophyll and high turbidity – here occurred with a delay after the spring tide  
370 (peaks in color changes in Fig. 6 happen after the apexes in the tidal range line). This time lag was between 4-5 days, when  
the tidal range was dropping and the system was close to entering a neap tide stage. Blue-green algae (Fig. 6f) were not a  
major contributor to total chlorophyll concentration (Figure 6e) in the Elbe Estuary. Maximum turbidity (Fig. 6g) and  
CDOM (Fig. 6h) were respectively lower and higher than in the Humber Estuary (Fig. 4g and 4h).

375

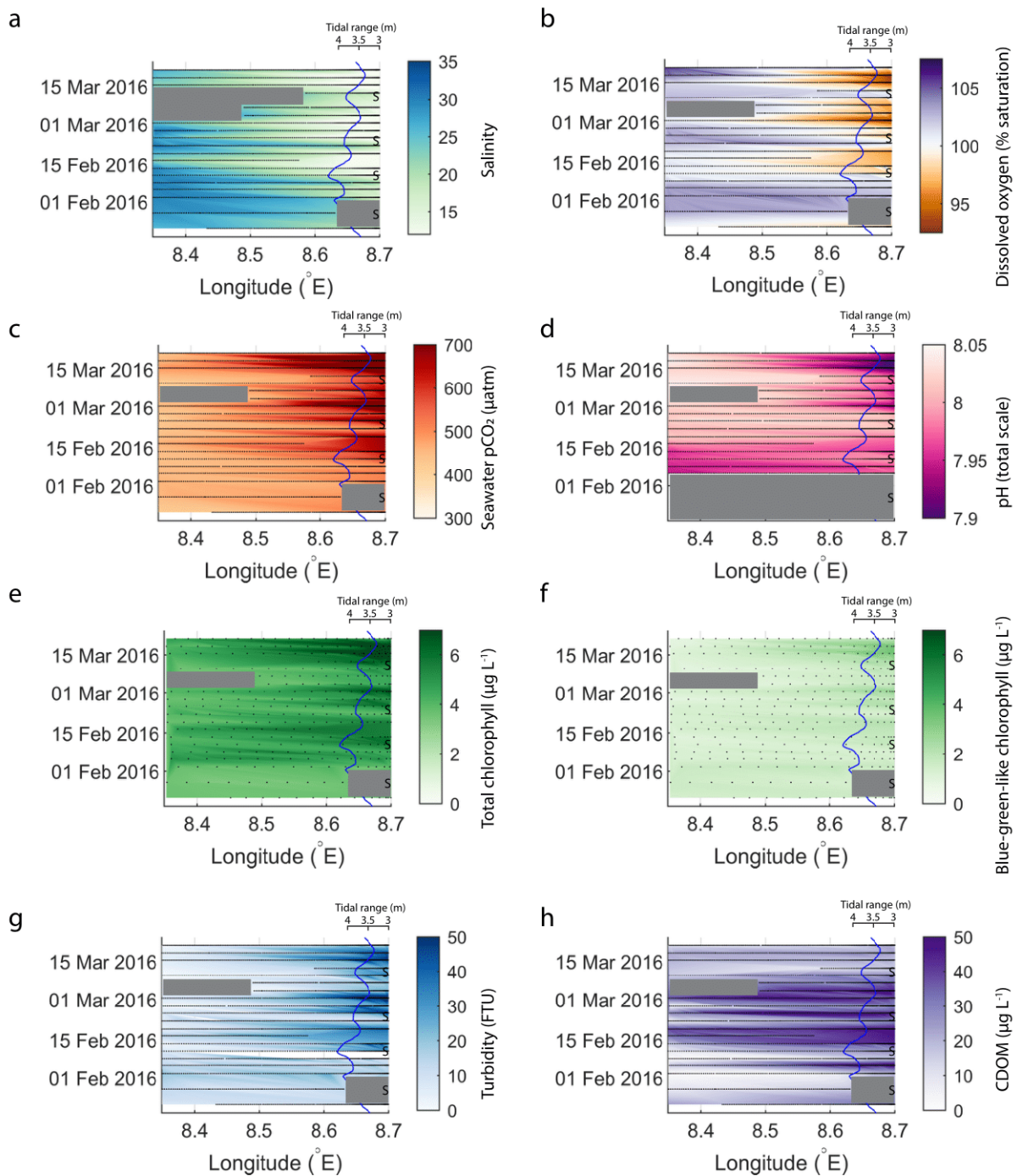


**Figure 6:** Variability in biogeochemical parameters in the outer Elbe Estuary during the same period as shown for the Humber Estuary in Fig. 4. The time/longitude coordinates of the measurements are shown in black. The tidal range is shown with the blue line and spring tides are indicated with “S” symbols. Note the reversal of the axis and change of tidal amplitude compared to Fig. 4. Large data gaps are

380 masked out with gray boxes. The variables shown are salinity (a), dissolved oxygen saturation (b),  $p\text{CO}_2$  (c), pH (d), total chlorophyll (e), blue-green-like chlorophyll (f), turbidity (g) and CDOM (h).

3.3 Comparing the Humber and Elbe outer estuaries

385 There are differences identified in the previous sections, so in Table 2, we provide a comparative summary of some correlations between the measured biogeochemical parameters in each outer estuary, as well as the relative phytoplankton algal class composition.

**Table 2:** Comparison of the Pearson correlation coefficients between seawater salinity and  $p\text{CO}_2$  and other FerryBox-measured essential ocean variables (EOV), respectively. Data from the whole 3-year time series divided between the two studied estuaries are used, 390 irrespective of tidal cycle. All correlation coefficients are significant at the 0.01 level and the number of measurements for each correlation is indicated. Also shown is the relative contribution of plankton species in the two outer estuaries. The total chlorophyll-a concentration is split into these four constituents.

	Humber	Elbe
	EOV-Salinity correlation coefficients	
Sea surface temperature	0.13 (n=39908)	0.25 (n=30202)
Seawater $p\text{CO}_2$	-0.82 (n=44757)	-0.57 (n=30592)
Total chlorophyll	-0.69 (n=5140)	-0.18 (n=3648)
Turbidity	-0.76 (n=35959)	-0.56 (n=25164)
CDOM	-0.42 (n=35861)	-0.68 (n=25164)
Dissolved Oxygen	-0.16 (n=43158)	-0.39 (n=30728)
	EOV- $p\text{CO}_2$ correlation coefficients	
Sea surface temperature	0.24 (n=40045)	-0.13 (n=30234)
Sea surface salinity	-0.82 (n=44757)	-0.57 (n=30592)
Total chlorophyll	0.55 (n=5154)	-0.34 (n=3621)
Turbidity	0.73 (n=36487)	0.52 (n=23975)
CDOM	0.39 (n=36403)	0.52 (n=23975)
Dissolved oxygen	-0.27 (n=43294)	-0.05 (n=30516)
	Phytoplankton class composition	
Diatoms	34.1%	53.3%
Blue-green-like algae	31.4%	16.4%
Green algae	31.0%	27.6%
Cryptophytes	3.2%	2.7%

395 The negative correlation coefficients between salinity and  $p\text{CO}_2$ , chlorophyll, turbidity, CDOM and oxygen suggest that all these parameters are higher in the low salinity endmember. Turbidity, CDOM and  $p\text{CO}_2$  are all higher in the low-salinity endmember than in the shelf sea and therefore positively correlated between each other in this estuarine setting. The relative contribution of blue-green-like algae was higher in the outer Humber Estuary than in the outer Elbe Estuary, where diatoms produced more than half of the observed phytoplankton chlorophyll.

### 400 3.4 Spring-neap effects on sea-air carbon fluxes at the land-sea interface

The seawater  $p\text{CO}_2$  in the outer Humber Estuary was higher than the atmospheric level, indicating that this estuarine outflow on the coast is a potential carbon source to the atmosphere. Moreover, during spring tides (Fig. 3c and 4c), the seawater  $p\text{CO}_2$  was much higher than during neap tides (at the most upstream location increasing from a mean of  $640 \pm 59 \mu\text{atm}$  to  $813 \pm 142 \mu\text{atm}$ ), leading to the estuary becoming a stronger potential source of carbon dioxide to the atmosphere, which we calculate here. If this spring-neap cycle difference is not considered, assessments of the role of estuaries in regional carbon budgets might underestimate the contribution of estuaries to the carbon cycle. We calculate average seawater  $p\text{CO}_2$  at the same locations as the box plot analysis (Fig. 3c) and use these averages and the average 2015-2017 atmospheric  $p\text{CO}_2$  ( $401 \pm 6.2 \mu\text{atm}$ ) to calculate sea-air carbon dioxide fluxes at each location and differentiate between the  $\text{CO}_2$  flux during neap and spring tides. We found no correlation between the daily averaged wind speed data and the tidal amplitude (Pearson's p-value of 0.45, tested on 181 data points in the first six months of 2017). Since there was no association of the higher  $p\text{CO}_2$  at spring tides with, for example, higher wind speeds, we therefore use the climatological average of the ERA5 wind speed in the Humber Estuary of  $6.9 \text{ m s}^{-1}$ . This isolates the investigated influence on sea-air carbon fluxes to tidally-driven seawater  $p\text{CO}_2$ , and not to wind speed. We calculate  $\text{CO}_2$  fluxes using the function *co2flux* available online (<https://github.com/mvdh7/co2flux>) (Humphreys et al., 2018) with the Wanninkhof (2014) gas transfer parameterization and the Weiss (1974) carbon dioxide solubility. At  $0.4^\circ\text{E}$ , where the riverine influence is limited, the average neap flux was  $3.6 \pm 3.7 \text{ mmol C m}^{-2} \text{ day}^{-1}$  and the average spring flux was  $5.0 \pm 5.5 \text{ mmol C m}^{-2} \text{ day}^{-1}$ . At the most upstream location, the increase between neap and spring tide averages was around 74%, from  $24.7 \pm 7.9$  to  $43.0 \pm 17.1 \text{ mmol C m}^{-2} \text{ day}^{-1}$ , respectively. The uncertainties of the flux calculations are propagated using the uncertainty of the atmospheric  $p\text{CO}_2$ , the standard deviation of the mean of the seawater  $p\text{CO}_2$  measurements at a certain location and tidal category, and the 20% uncertainty for the gas transfer velocity coefficient found by Wanninkhof (2014). Monthly averaged climatological wind speeds at our studied location range from  $5.3$  to  $8.4 \text{ m s}^{-1}$ , but we only use the annual average because our observations span multiple years and we do not differentiate by month. We defined an area the width of the river channel upstream and the width of the observational coverage offshore and integrated the fluxes over the resulting boxes. Based on our definition of spring and neap tide periods, these occupy around 50 days in one year. Therefore, based on the 2015-2017 conditions, the outer Humber Estuary releases  $2.1 \pm 1.2 \text{ Gg C}$  per year to the atmosphere during neap tide periods, compared to  $3.4 \pm 2.1 \text{ Gg}$

C per year during spring tide periods, changing the area-integrated sea-air flux of this estuary during spring tide by over 60%. This change does not refer to the rest of the 265 days during transitional tidal periods.

## 4 Discussion

### 4.1 Drivers of biogeochemical variability

430 The spring-neap tidal cycles influence the strength of the potential carbon source to the atmosphere in outer estuaries, accounting for the largest variability in  $p\text{CO}_2$  on timescales longer than semi-diurnally, based on Fourier Transform analysis (Fig. 2c). In outer estuaries like the Humber Estuary, this results in a stronger (by over 60%) area-integrated carbon source to the atmosphere during spring tides compared to neap tide conditions. In our observations, the periodicity of the biogeochemical changes, including salinity, turbidity, seawater  $p\text{CO}_2$ , dissolved oxygen saturation and chlorophyll, largely  
435 aligns with the spring-neap tidal cycle periodicity, suggesting that this is an essential modulator of carbon cycling and ecosystem parameters at the land-sea interface. Below, we identified the processes that likely force the outer Humber Estuary system to experience the observed spring-neap  $p\text{CO}_2$  tidal variability.

Estuaries are generally considered to be net heterotrophic environments and sources of carbon to the atmosphere (Smith and  
440 Hollibaugh, 1993; Chen and Borges, 2009; Cai, 2010; Canuel and Hardison, 2016; Volta et al., 2016). In contrast, shelf seas, such as the North Sea, are generally net autotrophic and their in situ primary production is driven by the riverine nutrient loads (Kühn et al., 2010). Therefore, the outer estuary region is characterized by large gradients, not only in salinity, but also in other biogeochemical parameters, such as nutrient concentrations and pH (Kerimoglu et al., 2018). The observed spring tide oxygen undersaturation and increase in seawater  $p\text{CO}_2$  in the outer Humber Estuary are indicative of a net heterotrophic  
445 environment. While higher chlorophyll concentrations were also observed during spring tides, we postulate that this is not locally-produced biomass and does not lead to a decrease in seawater  $p\text{CO}_2$  via autochthonous primary production. Water mass movement simulations (Fig. S4) suggest that the chlorophyll observed in the outer estuary during spring tides could be allochthonous and could be produced in the river or inner estuary. The similarity of the observed chlorophyll fluorescence to blue-green algae-like material also hints towards a more inland origin of the organic matter. The cells could be damaged in  
450 contact with salt water and the chlorophyll released can be observed by our instruments (Yang et al., 2020). The Humber Estuary is generally turbid and exhibits an increase of at least 18% in turbidity during spring tides. These conditions do not facilitate local primary production that would lower the seawater  $p\text{CO}_2$ .

### 4.2 Organic matter transformations at the estuary-sea interface

455 In the outer estuaries of Humber and Elbe, the negative correlation between CDOM and salinity and the positive correlation between CDOM and  $p\text{CO}_2$  (Table 2) confirm our existing knowledge about the origin and estuarine distribution of this

component of the riverine dissolved matter. For instance, CDOM was strongly negatively correlated to salinity and showed a conservative behavior indicative of a terrestrial source in a study of Norwegian rivers (Frigstad et al., 2020). Dissolved organic carbon, for which CDOM can be used as a proxy, can feature a variety of behaviors in estuaries depending on flushing time and variations in the source of organic matter (Bowers and Brett, 2008;García-Martín et al., 2021). What is particularly noteworthy in our study is that higher CDOM concentrations were usually associated with the neap tides in both estuaries (Fig. 3h and 5h). This suggests that the fraction of organic carbon in the dissolved form in the outer estuary is larger during the neap tide periods than during spring tides. At the same time, the inorganic carbon in the form of dissolved carbon dioxide also varies with the spring-neap cycle (Fig. 3c and 5c). This has an impact on the quantity and type of lateral carbon transport across the LSI. On a shorter timescale of variability, Chen et al. (2016) found examples of higher CDOM during the ebb tide phase, when phytoplankton is not dispersed by the more dynamic conditions at high tide. Resuspension of bottom sediments at spring tide might also suppress the effect of terrestrial sources, usually the main input of CDOM to the estuary (Ferreira et al., 2014). High CDOM can also come from the bacterial degradation of phytoplankton-derived detritus (Astoreca et al., 2009), and high turbidity can protect the detritus from photodegradation (Juhls et al., 2019), although the switch between tidal conditions might be too fast for this process to play a major role. We postulate that, in tidally-driven outer estuaries, cycling between the spring and neap tidal stages provides favorable conditions for dissolved organic material to be either brought to the surface from the benthos or transported to the outer estuary from further inshore during spring tides and subsequently transformed during neap tides into a measurable form by our CDOM instrument.

475



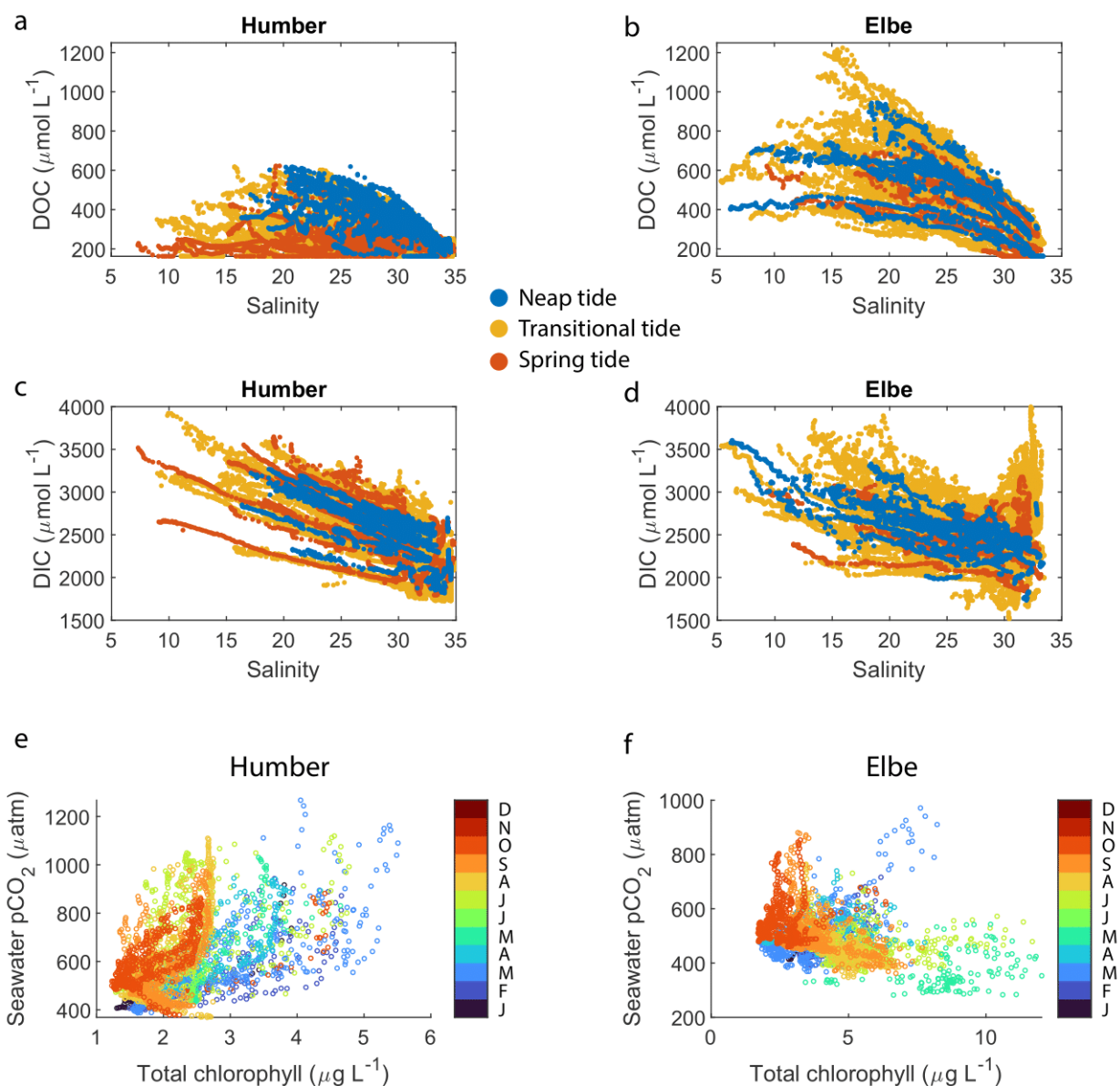


**Figure 7:** Estimated dissolved organic carbon (a) and (b) and dissolved inorganic carbon (c) and (d) concentrations in the Humber and Elbe estuaries, respectively plotted against salinity and color-separated according to the spring-neap tidal cycle. Relationship between seawater  $p\text{CO}_2$  and total chlorophyll in the outer estuaries of the Humber (e) and Elbe (f). The data points are colored by month.

480

The addition of dissolved organic matter in the outer estuary is supported by the positive non-linear distribution of CDOM-derived DOC against a theoretical linear salinity gradient when assuming conservative mixing (Fig. 7a,b), indicating a

source of DOC within the estuary, at the land-sea interface. Although we do not capture salinities for the freshwater endmember, some data points in the middle of the outer estuary lie above the line connecting the marine term to the lowest available salinity. The DOC enhancement at mid-salinities was pronounced during neap tides in the Humber; for example, at salinities of  $22.5 \pm 1$ , the mean spring tide DOC concentration was  $297 \pm 106 \mu\text{mol L}^{-1}$ , while the mean neap tide DOC was  $467 \pm 86 \mu\text{mol L}^{-1}$ . There was no similar pattern in the Elbe, where at the same salinities as in the Humber example, the mean DOC concentrations were higher than in the Humber, but statistically indistinguishable between spring and neap tide. The ratio between the forms of dissolved carbon favored the inorganic one. At a salinity of  $20 \pm 1$ , DOC was approximately 10% of the total dissolved carbon pool in the Humber and 18% in the Elbe. This is slightly lower than the 20% average in UK rivers (Jarvie et al., 2017). The calculated DOC concentrations for the outer Humber Estuary were higher than the Humber riverine end-member used by García-Martín et al. (2021), but in the range reported by Tipping et al. (1997) for the Humber and by Williamson et al. (2023) for the Trent tributary, and actually lower than the Humber value reported by Painter et al. (2018) and Dai et al. (2012). The Elbe DOC concentrations were within the range of measurements conducted by the Flussgebietsgemeinschaft Elbe at the Cuxhaven station (FGG, River Basin Community; <https://www.fgg-elbe.de/elbe-datenportal.html>). The linear empirical DOC:CDOM relationship we used has a high intercept of  $162 \mu\text{mol L}^{-1}$ . This means that there is DOC in the water even when the CDOM fluorescence readings are 0. The fluorometer can only detect a specific fluorescent chemical group and nothing that does not fluoresce. Furthermore, in a study in the coastal Arctic, another empirical relationship between DOC and CDOM quinine sulphate fluorescence found a similarly high intercept of  $110 \mu\text{mol L}^{-1}$  (Pugach et al., 2018). Mid-estuary non-conservative DOC enhancement, such as in our study, was also found by McKenna (2004), who attributed it to phytoplankton-derived autochthonous inputs. In the studied estuaries, the measured high chlorophyll concentrations coincide with low oxygen, so the primary production happens elsewhere, and the DOC we observe at neap tides is a result of transformations of allochthonous organic matter. Alternatively, the high turbidity during spring tides could prevent our fluorescence-based instrument to detect the entire CDOM present in the surface waters.

505

The calculated DIC on the Elbe side was higher than other reported values in the Elbe Estuary or German Bight (Reimer et al., 1999; Rewrie et al., 2023b), but similar relationships with salinity in the outer Elbe Estuary were observed at certain times during our period of observations, as shown in the Supplementary Material provided by Rewrie et al. (2023b). The DIC values reported here are however subject to the combined uncertainties of the measurements and the calculations. The  $p\text{CO}_2$  – pH pair, which we used due to our data availability, has the highest calculation uncertainty, with a carbonate ion squared combined standard uncertainty of nearly  $40 \mu\text{mol kg}^{-1}$  (Orr et al., 2018). There were also DIC data in the Elbe outflow at salinities higher than 30 which did not follow the salinity relationship of the other data points (Fig. 7d). These data were calculated using measurements from July-August 2017, a period when another study found elevated DIC concentrations in the Elbe Estuary (Rewrie et al., 2023a).

515

Having observed the spring-neap influence on the concentrations of dissolved carbon fractions, we used the average DOC and DIC concentrations at the most upstream locations sampled (westernmost longitude group in the outer Humber Estuary box plot and easternmost longitude group in the outer Elbe Estuary) to provide a quantitative assessment of lateral land-sea fluxes (Table 3). We use average literature discharge for the Humber and 2016-2017 measured discharge for the Elbe (FGG) and adjusted for tributary influence based on Amann et al. (2012). We also employ a similar methodology to the vertical carbon flux calculations in Section 3.4 to calculate the mass of carbon transported during the spring or neap tide events in an average year, excluding the other 265 days during transitional tide periods. The lateral flux of DOC is 43% and 20% higher during neap tide in the Humber and Elbe outer estuaries, respectively. The lateral flux of DIC in the Elbe also increases during neap tides, by 11%, but in the Humber, the DIC flux decreases by 4% during neap tides. All the differences are statistically significant at the 5% level, tested with a two-sample t-test. We also provide the equivalent mass transport out of our estuaries during the two different tide events. For context, Kitidis et al. (2019) estimate a whole northwestern European Shelf DOC and DIC riverine flux of 2.1 and 18.9 Tg C yr<sup>-1</sup> respectively upstream of the estuaries and 2.6 and 2.0 Tg C yr<sup>-1</sup> respectively in the outer estuaries.

**Table 3:** Average ( $\pm$  standard deviation) lateral organic and inorganic carbon fluxes from the two outer estuaries depending on the spring-neap tidal stage.

	Land-sea lateral DOC flux		Land-sea lateral DIC flux	
	(mol s <sup>-1</sup> )	(Tg in 50 days)	(mol s <sup>-1</sup> )	(Tg in 50 days)
Humber neap tide	103 $\pm$ 26	0.005 $\pm$ 0.001	716 $\pm$ 44	0.037 $\pm$ 0.002
Humber spring tide	72 $\pm$ 28	0.004 $\pm$ 0.001	744 $\pm$ 69	0.039 $\pm$ 0.003
Elbe neap tide	398 $\pm$ 109	0.021 $\pm$ 0.006	1912 $\pm$ 177	0.099 $\pm$ 0.009
Elbe spring tide	332 $\pm$ 68	0.017 $\pm$ 0.004	1716 $\pm$ 178	0.089 $\pm$ 0.009

There are also differences between the two outer estuaries related to the dissolved oxygen and chlorophyll measurements. In an open-marine setting, oxygen and  $p\text{CO}_2$  are strongly inversely correlated, a function of primary production and respiration (DeGrandpre et al., 1997). In coastal regions however, there are distinct  $p\text{CO}_2$ -to-dissolved oxygen relationships due to variability in Revelle factors and different sea-air equilibration times (Zhai et al., 2009). Both in the Humber and Elbe outer estuaries,  $p\text{CO}_2$  and dissolved oxygen were inversely correlated, although in the Elbe, the correlation was weak. Combining this with the direct versus inverse correlations between  $p\text{CO}_2$  and chlorophyll in the Humber and Elbe, respectively (Table 2), indicates that the two outer estuaries have a different metabolic behavior. Having high chlorophyll coinciding with low oxygen and high  $p\text{CO}_2$  suggests that the chlorophyll was not locally produced in the outer Humber Estuary. Instead, this location is the site where chlorophyll-containing organic matter likely produced upstream in the estuary was typically remineralized. During the summer and fall seasons however, in months when the minimum seawater temperature was higher than 12.5 °C, the relationship was closer to what is expected during conventional marine primary production (orange tone

545 colors at  $p\text{CO}_2$  levels below 550  $\mu\text{atm}$  in Fig. 7e). When combining the whole-year data and including the very high  $p\text{CO}_2$   
brackish water-influenced measurements, the usual negative correlation changes. Due to the location of the ports, the ship  
was not entering the Elbe Estuary main channel as far upstream as the Humber Estuary (Fig. 1d and 1c, respectively), so in  
the outer Elbe Estuary, we were observing a more typically-marine behavior (Fig. 7f). The outer Humber Estuary is highly  
turbid and a location of organic matter degradation, while the organic matter in the Elbe is processed further upstream in the  
estuary, allowing the outer Elbe Estuary to take up some carbon through organic matter production, leading to the  
550 differences in Fig. 7e,f.

Some studies found that higher chlorophyll concentrations in estuaries are associated with neap tides, when the water  
residence time is longer and conditions are calmer (Lucas et al., 1999; Trigueros and Orive, 2000; Domingues et al.,  
2010; Flores-Melo et al., 2018). Production from phytoplankton is limited by light and nutrient availability. In estuarine  
555 settings, the high nutrient availability means the peak chlorophyll usually coincides with peak solar irradiance (Jakobsen and  
Markager, 2016). Over a longer seasonal term, this guides the onset of spring plankton blooms. On shorter time scales, the  
optimal conditions for primary production occur at the onset of stratification, as the estuary is shifting towards a neap tide  
stage, but also benefiting from the extra nutrients brought to the surface during the previous dynamic spring tide stage. This  
succession of events is what likely led to our outer Elbe Estuary observations (Fig. 6e). In contrast to the paradigm of high  
560 chlorophyll at neap tides, and similar to what we observed in the Humber Estuary, the Tagus estuary in Portugal showed  
higher biomass during spring tides (Cereja et al., 2021). This was caused by resuspension of sediments and mixing of  
microphytobenthos into the water column, a phenomenon also described by Macintyre and Cullen (1996). The high  
chlorophyll concentrations we measured during spring tide in the Humber Estuary either have a similar origin, or  
alternatively, come from somewhere else and are therefore not locally-produced.

565 The dominant phytoplankton class were diatoms, while green algae made up around 30% of the total chlorophyll in both  
estuaries. However, the relative abundance of blue-green-like algae in the Humber was nearly double to the Elbe (31%  
versus 16%, respectively, Table 2). This was mainly driven by the increasing blue-green-like algae chlorophyll  
concentrations at spring tides (Fig. 3f and 4f). Blue-green algae, or cyanobacteria, are microscopic photosynthetic  
570 prokaryotes, which are more common in freshwater (Iriarte and Purdie, 1993). Their occurrence in the North Sea is usually  
restricted to the Skagerrak-Norwegian Channel region (Brandsma et al., 2013). Although this study focuses on estuary-  
influenced regions, and cyanobacteria can actually dominate the plankton biomass in estuaries or be in phase with tidally-  
driven stratification events (Eldridge and Sieracki, 1993; Murrell and Lores, 2004), there are likely no relevant concentrations  
of cyanobacteria in this region of the North Sea. The instrument is possibly interpreting the fluorescence excitation from a  
575 slightly different algal group as that coming from cyanobacteria. During a usual open-ocean spring bloom, the most efficient  
nutrient-utilizing plankton are the diatoms (Flores-Melo et al., 2018). What we could be observing in the outer Humber  
Estuary is a smaller scale version of this effect, where diatoms are outcompeting other algae during neap tides, and the latter

are utilizing the spring tide niche for their development (Rocha et al., 2002). Alternatively, if the chlorophyll we observed at spring tides was not autochthonous, our observations could be influenced by how refractory the material is. Different phytoplankton species release varying dissolved organic matter, and the organic matter from the blue-green-like algae is more resistant to degradation by microorganisms, therefore observable by our instruments (Osterholz et al., 2021).

### 4.3 Models versus observations

The carbon flux to the atmosphere in the outer Humber Estuary ranged between 3.6 mmol m<sup>-2</sup> day<sup>-1</sup> offshore at neap tide and 43.0 mmol m<sup>-2</sup> day<sup>-1</sup> nearshore at Immingham at spring tide. This places the outer estuary outgassing between estimates for the Southern North Sea at 2.1 mmol m<sup>-2</sup> day<sup>-1</sup> (Prowe et al., 2009) and Northwest European Shelf estuaries as a whole at 54-170 mmol m<sup>-2</sup> day<sup>-1</sup> (Kitidis et al., 2019), but emphasizes the proper accounting of this flux with consideration to the spring-neap cycle. Excess dissolved inorganic carbon produced by respiration and remineralization makes estuaries carbon sources to the atmosphere. A study found that about 60% of the heterotrophic carbon in an estuary was lost by evasion to the atmosphere (Raymond et al., 2000). We show here that this evasion happens along a gradient and varies according to the different stages in the tidal spring-neap cycle, and therefore the estuarine influence on nearshore seawater *p*CO<sub>2</sub> can extend further offshore than expected, depending on a reference point, with influence on regional flux calculations.

The importance of the LSI is now a more prominent topic in the literature and the knowledge gaps are identified as research priorities (Legge et al., 2020). The areas adjacent to river mouths were necessary to be considered when closing the carbon budget of the Baltic Sea (Kuliński et al., 2011). We have evidence that high *p*CO<sub>2</sub> waters can be advected seaward due to river outflow and tidal exchanges (Reimer et al., 2017). The Southern Bight of the North Sea was a carbon sink over an annual integration with a flux of 2.27 mmol m<sup>-2</sup> day<sup>-1</sup>, but including estuarine plumes in the calculation decreased the carbon uptake potential to 1.78 mmol m<sup>-2</sup> day<sup>-1</sup> (Schiettecatte et al., 2007). In spite of all this, some Earth System Models still lack the implementation of estuarine systems because of the computational constraints of reproducing their variability (Regnier et al., 2013). We observed this effect in particular for the outer Humber Estuary region in a previous study (Macovei et al., 2022). A model that correctly replicated high chlorophyll observations in the central North Sea also replicated the associated decrease in sea surface *p*CO<sub>2</sub>. However, the same model underestimated seawater *p*CO<sub>2</sub> in the area of influence of the Humber Estuary, likely since it associated the high chlorophyll recorded during spring tides with carbon dioxide drawdown. We show here that these variables are not necessarily negatively-correlated in outer estuaries (Fig. 7e, Table 2), where conflicting processes occur, and this can lead to incorrect CO<sub>2</sub> sea-air flux estimates. As all coastal environments, outer estuaries are also vulnerable to anthropogenically-driven climate change, and uncertainty regarding the direction of change remains. Resolving the competing and rapidly varying processes of the future river-influenced coastal seas first requires a thorough understanding of the present-day processes.

610 **5 Conclusion**

Estuaries are complex environments, with tides inducing large variability in biogeochemical parameters. Here, we used the high measurement frequency and multitude of sensors that FerryBoxes installed on a Ship-of-Opportunity allow and described the spring-neap tidal variability in two large outer estuaries draining into the North Sea and find that spring-neap variability plays an important role in modulating carbon fluxes at the land-ocean interface. Moreover, this study demonstrates that the spring-neap variability usually seen at a fixed-point station can also be observed from a regularly transiting ship, with the added benefit of determining the spatial extent of the estuarine influence on the coast. In the macrotidal, well-mixed Humber Estuary, seawater  $p\text{CO}_2$  was up to 21% higher during the more turbid spring tides, under heterotrophic conditions, as shown by the widespread oxygen undersaturation. At the most upstream location in our study area in the outer Humber Estuary, the sea-to-air carbon dioxide flux increased from  $24.7 \pm 7.9 \text{ mmol C m}^{-2} \text{ day}^{-1}$  during neap tides to  $43.0 \pm 17.1 \text{ mmol C m}^{-2} \text{ day}^{-1}$  during spring tides. Lateral dissolved organic carbon flux, on the other hand, increased from  $72 \pm 28 \text{ mol s}^{-1}$  during spring tides to  $103 \pm 26 \text{ mol s}^{-1}$  during neap tides. This means that the strength of carbon evasion from macrotidal, well-mixed estuaries could be misrepresented in models and budget calculations if the fortnightly tidal cycle is not considered. Moreover, we showed that the estuarine outflow influence stretched at least 7 km offshore and this is sometimes not correctly reproduced in models, as observed by Macovei et al. (2022) using another dataset. We described the competing processes forcing  $p\text{CO}_2$  in the outer estuaries and showed how different biogeochemical parameters correlate. Spring tide conditions were associated with higher phytoplankton biomass, mainly driven by blue-green-like algae, which were remineralized in the outer estuary. Neap tide conditions were associated with higher CDOM, produced in the estuary, likely derived from allochthonous material. The dissolved carbon pool in both outer estuaries studied here was dominated by the inorganic form, with DOC being less than 20% of the total. However, indications of non-conservative addition of DOC into the outer estuary were observed at mid-salinities, in particular in the Humber, where DOC concentrations during neap tides were 57% higher than during spring tide, altering the lateral flux ratio of dissolved organic to dissolved inorganic carbon across the LSI depending on the spring-neap cycle. The conclusions presented describe well-mixed tidal outer estuaries, and this is an important first step in understanding the drivers of biogeochemical variability in classical estuaries before the complexity of global-scale land-sea interactions are assessed. Although the North Sea is one of the most studied marginal seas, its biogeochemistry is still not fully parameterised for integration into models, in particular in the freshwater influenced areas. With this study, we are following the call of the community by providing observations at the land-ocean interface and we our results can be used to improve the performance of regional biogeochemical models, with ulterior upscaling into Earth System Models and carbon budgeting.

640 **Code availability**

Code is available upon request to the corresponding author.

## Data availability

Quality controlled temperature, salinity and  $p\text{CO}_2$  data obtained by this SOO are now publicly available on the Pangaea repository (<https://doi.org/10.1594/PANGAEA.930383>). All data are also available in the European FerryBox Database  
645 (<https://ferrydata.hereon.de>). Data are also available upon request to the corresponding author.

## Author contribution

**VAM:** Conceptualization, Formal analysis, Writing – Original Draft, Visualization

**LCVR:** Resources, Writing – Review and Editing

**RR:** Resources, Writing – Review and Editing

650 **YGV:** Conceptualization, Writing – Review and Editing, Supervision, Funding acquisition.

## Competing interests

The authors declare that they have no conflict of interest.

## Acknowledgements

We thank two anonymous reviewers whose comments helped to improve and clarify the manuscript. We would like to thank  
655 the DFDS Seaways and CLdN RoRo & Cobelfret Ferries companies, as well as the captains, officers and crews of *Hafnia Seaways* for facilitating our measurements on board their ship. Our sincere gratefulness goes to the FerryBox group engineers and scientists who installed the instruments and regularly serviced them. We thank Kerstin Heymann for the HPLC chlorophyll analysis. FerryBox activities were funded by the Helmholtz Association. Measurements during the RV *Heincke* campaign in 2013 were conducted under the grant number AWI-HE407-00. Funding for this research was provided  
660 through the Helmholtz Association EU Partnering “SEA-ReCap – Research capacity building for healthy, productive and resilient seas” project and the Helmholtz Association “Changing Earth” program, as well as by project Horizon Europe project LandSeaLot, Grant Agreement number 101134575.

## References

Alduchov, O. A., and Eskridge, R. E.: Improved Magnus Form Approximation of Saturation Vapor Pressure, Journal of Applied Meteorology, 35, 601-609, 10.1175/1520-0450(1996)035<0601:IMFAOS>2.0.CO;2, 1996.  
665 Amann, T., Weiss, A., and Hartmann, J.: Carbon dynamics in the freshwater part of the Elbe estuary, Germany: Implications of improving water quality, Estuarine, Coastal and Shelf Science, 107, 112-121, <https://doi.org/10.1016/j.ecss.2012.05.012>, 2012.

- Artioli, Y., Blackford, J. C., Butenschön, M., Holt, J. T., Wakelin, S. L., Thomas, H., Borges, A. V., and Allen, J. I.: The carbonate system in the North Sea: Sensitivity and model validation, *Journal of Marine Systems*, 102-104, 1-13, 10.1016/j.jmarsys.2012.04.006, 2012.
- Astoreca, R., Rousseau, V., and Lancelot, C.: Coloured dissolved organic matter (CDOM) in Southern North Sea waters: Optical characterization and possible origin, *Estuarine, Coastal and Shelf Science*, 85, 633-640, <https://doi.org/10.1016/j.ecss.2009.10.010>, 2009.
- Baschek, B., Schroeder, F., Brix, H., Riethmüller, R., Badewien, T. H., Breitbach, G., Brugge, B., Colijn, F., Doerffer, R., Eschenbach, C., Friedrich, J., Fischer, P., Garthe, S., Horstmann, J., Krasemann, H., Metfies, K., Merckelbach, L., Ohle, N., Petersen, W., Proffrock, D., Rottgers, R., Schluter, M., Schulz, J., Schulz-Stellenfleth, J., Stanev, E., Staneva, J., Winter, C., Wirtz, K., Wollschläger, J., Zielinski, O., and Ziemer, F.: The Coastal Observing System for Northern and Arctic Seas (COSYNA), *Ocean Science*, 13, 379-410, 10.5194/os-13-379-2017, 2017.
- Bauer, J. E., Cai, W.-J., Raymond, P. A., Bianchi, T. S., Hopkinson, C. S., and Regnier, P. A. G.: The changing carbon cycle of the coastal ocean, *Nature*, 504, 61-70, 10.1038/nature12857, 2013.
- Borges, A. V.: Do we have enough pieces of the jigsaw to integrate CO<sub>2</sub> fluxes in the coastal ocean?, *Estuaries*, 28, 3-27, 10.1007/BF02732750, 2005.
- Bourgeois, T., Orr, J. C., Resplandy, L., Terhaar, J., Ethé, C., Gehlen, M., and Bopp, L.: Coastal-ocean uptake of anthropogenic carbon, *Biogeosciences*, 13, 4167-4185, 10.5194/bg-13-4167-2016, 2016.
- Bowers, D. G., and Brett, H. L.: The relationship between CDOM and salinity in estuaries: An analytical and graphical solution, *Journal of Marine Systems*, 73, 1-7, <https://doi.org/10.1016/j.jmarsys.2007.07.001>, 2008.
- Brandsma, J., Martínez, J. M., Slagter, H. A., Evans, C., and Brussaard, C. P. D.: Microbial biogeography of the North Sea during summer, *Biogeochemistry*, 113, 119-136, 10.1007/s10533-012-9783-3, 2013.
- Brasse, S., Nellen, M., Seifert, R., and Michaelis, W.: The carbon dioxide system in the Elbe estuary, *Biogeochemistry*, 59, 25-40, 10.1023/A:1015591717351, 2002.
- Burson, A., Stomp, M., Akil, L., Brussaard, C. P. D., and Huisman, J.: Unbalanced reduction of nutrient loads has created an offshore gradient from phosphorus to nitrogen limitation in the North Sea, *Limnology and Oceanography*, 61, 869-888, 10.1002/lno.10257, 2016.
- Butenschön, M., Clark, J., Aldridge, J. N., Allen, J. I., Artioli, Y., Blackford, J., Bruggeman, J., Cazenave, P., Ciavatta, S., Kay, S., Lessin, G., van Leeuwen, S., van der Molen, J., de Mora, L., Polimene, L., Saille, S., Stephens, N., and Torres, R.: ERSEM 15.06: a generic model for marine biogeochemistry and the ecosystem dynamics of the lower trophic levels, *Geosci. Model Dev.*, 9, 1293-1339, 10.5194/gmd-9-1293-2016, 2016.
- Cadier, M., Gorgues, T., Lhelguen, S., Sourisseau, M., and Memery, L.: Tidal cycle control of biogeochemical and ecological properties of a macrotidal ecosystem, *Geophysical Research Letters*, 44, 8453-8462, <https://doi.org/10.1002/2017GL074173>, 2017.
- Cai, W.-J.: Estuarine and Coastal Ocean Carbon Paradox: CO<sub>2</sub> Sinks or Sites of Terrestrial Carbon Incineration?, *Annual Review of Marine Science*, 3, 123-145, 10.1146/annurev-marine-120709-142723, 2010.
- Cai, W.-J., Feely, R. A., Testa, J. M., Li, M., Evans, W., Alin, S. R., Xu, Y.-Y., Pelletier, G., Ahmed, A., Greeley, D. J., Newton, J. A., and Bednaršek, N.: Natural and Anthropogenic Drivers of Acidification in Large Estuaries, *Annual Review of Marine Science*, 13, 23-55, 10.1146/annurev-marine-010419-011004, 2021.
- Cai, W. J., and Wang, Y.: The chemistry, fluxes, and sources of carbon dioxide in the estuarine waters of the Satilla and Altamaha Rivers, Georgia, *Limnology and Oceanography*, 43, 657-668, 1998.
- Callies, U., Plüß, A., Kappenberg, J., and Kapitza, H.: Particle tracking in the vicinity of Helgoland, North Sea: a model comparison, *Ocean Dyn.*, 61, 2121-2139, 10.1007/s10236-011-0474-8, 2011.
- Callies, U.: Sensitive dependence of trajectories on tracer seeding positions – coherent structures in German Bight backward drift simulations, *Ocean Sci.*, 17, 527-541, 10.5194/os-17-527-2021, 2021.
- Callies, U., Kreus, M., Petersen, W., and Voynova, Y. G.: On Using Lagrangian Drift Simulations to Aid Interpretation of in situ Monitoring Data, *Frontiers in Marine Science*, 8, 769, 2021.
- Canuel, E. A., and Hardison, A. K.: Sources, Ages, and Alteration of Organic Matter in Estuaries, *Annual Review of Marine Science*, 8, 409-434, 10.1146/annurev-marine-122414-034058, 2016.



- Cave, R. R., Ledoux, L., Turner, K., Jickells, T., Andrews, J. E., and Davies, H.: The Humber catchment and its coastal area: from UK to European perspectives, *Science of The Total Environment*, 314-316, 31-52, [https://doi.org/10.1016/S0048-9697\(03\)00093-7](https://doi.org/10.1016/S0048-9697(03)00093-7), 2003.
- 720 Cereja, R., Brotas, V., Cruz, J. P. C., Rodrigues, M., and Brito, A. C.: Tidal and Physicochemical Effects on Phytoplankton Community Variability at Tagus Estuary (Portugal), *Frontiers in Marine Science*, 8, 2021.
- Chegini, F., Holtermann, P., Kerimoglu, O., Becker, M., Kreuz, M., Klingbeil, K., Gräwe, U., Winter, C., and Burchard, H.: Processes of Stratification and Destratification During An Extreme River Discharge Event in the German Bight ROFI, *Journal of Geophysical Research: Oceans*, 125, e2019JC015987, <https://doi.org/10.1029/2019JC015987>, 2020.
- 725 Chen, C.-T. A., and Borges, A. V.: Reconciling opposing views on carbon cycling in the coastal ocean: Continental shelves as sinks and near-shore ecosystems as sources of atmospheric CO<sub>2</sub>, *Deep Sea Research Part II: Topical Studies in Oceanography*, 56, 578-590, 10.1016/j.dsr2.2009.01.001, 2009.
- Chen, J., Ye, W., Guo, J., Luo, Z., and Li, Y.: Diurnal Variability in Chlorophyll-a, Carotenoids, CDOM and SO<sub>4</sub><sup>2-</sup> Intensity of Offshore Seawater Detected by an Underwater Fluorescence-Raman Spectral System. In: *Sensors*, 7, 2016.
- 730 Clargo, N. M., Salt, L. A., Thomas, H., and de Saar, H. J. W.: Rapid increase of observed DIC and pCO<sub>2</sub> in the surface waters of the North Sea in the 2001-2011 decade ascribed to climate change superimposed by biological processes, *Marine Chemistry*, 177, 566-581, 10.1016/j.marchem.2015.08.010, 2015.
- Dähne, K., Bahlmann, E., and Emeis, K.: A nitrate sink in estuaries? An assessment by means of stable nitrate isotopes in the Elbe estuary, *Limnology and Oceanography*, 53, 1504-1511, <https://doi.org/10.4319/lo.2008.53.4.1504>, 2008.
- 735 Dai, M., Yin, Z., Meng, F., Liu, Q., and Cai, W.-J.: Spatial distribution of riverine DOC inputs to the ocean: an updated global synthesis, *Current Opinion in Environmental Sustainability*, 4, 170-178, <https://doi.org/10.1016/j.cosust.2012.03.003>, 2012.
- Dai, M., Su, J., Zhao, Y., Hofmann, E. E., Cao, Z., Cai, W.-J., Gan, J., Lacroix, F., Laruelle, G. G., Meng, F., Müller, J. D., Regnier, P. A. G., Wang, G., and Wang, Z.: Carbon Fluxes in the Coastal Ocean: Synthesis, Boundary Processes, and Future Trends, *Annual Review of Earth and Planetary Sciences*, 50, 593-626, 10.1146/annurev-earth-032320-090746, 2022.
- 740 DeGrandpre, M. D., Hammar, T. R., Wallace, D. W. R., and Wirick, C. D.: Simultaneous mooring-based measurements of seawater CO<sub>2</sub> and O<sub>2</sub> off Cape Hatteras, North Carolina, *Limnology and Oceanography*, 42, 21-28, <https://doi.org/10.4319/lo.1997.42.1.0021>, 1997.
- Dickson, A., Wesolowski, J. D., Palmer, D., and Mesmer, E. R.: Dissociation Constant of Bisulfate Ion in Aqueous Sodium Chloride Solutions to {250°C}, 1990.
- 745 Domingues, R. B., Anselmo, T. P., Barbosa, A. B., Sommer, U., and Galvão, H. M.: Tidal Variability of Phytoplankton and Environmental Drivers in the Freshwater Reaches of the Guadiana Estuary (SW Iberia), *International Review of Hydrobiology*, 95, 352-369, <https://doi.org/10.1002/iroh.201011230>, 2010.
- Dyer, K. R., and Moffat, T. J.: Fluxes of suspended matter in the East Anglian plume Southern North Sea, *Continental Shelf Research*, 18, 1311-1331, [https://doi.org/10.1016/S0278-4343\(98\)00045-4](https://doi.org/10.1016/S0278-4343(98)00045-4), 1998.
- 750 Eldridge, P. M., and Sieracki, M. E.: Biological and hydrodynamic regulation of the microbial food web in a periodically mixed estuary, *Limnology and Oceanography*, 38, 1666-1679, <https://doi.org/10.4319/lo.1993.38.8.1666>, 1993.
- Ferreira, A., Ciotti, Á. M., and Coló Gianni, M. F.: Variability in the light absorption coefficients of phytoplankton, non-algal particles, and colored dissolved organic matter in a subtropical bay (Brazil), *Estuarine, Coastal and Shelf Science*, 139, 127-136, <https://doi.org/10.1016/j.ecss.2014.01.002>, 2014.
- 755 Flores-Melo, X., Schloss, I. R., Chavanne, C., Almandoz, G. O., Latorre, M., and Ferreyra, G. A.: Phytoplankton Ecology During a Spring-Neap Tidal cycle in the Southern Tidal Front of San Jorge Gulf, Patagonia, *OCEANOGRAPHY*, 31, 70-80, 10.5670/oceanog.2018.412, 2018.
- Frigstad, H., Kaste, Ø., Deininger, A., Kvalsund, K., Christensen, G., Bellerby, R. G. J., Sørensen, K., Norli, M., and King, A. L.: Influence of Riverine Input on Norwegian Coastal Systems, *Frontiers in Marine Science*, 7, 332, 2020.
- 760 García-Martín, E. E., Sanders, R., Evans, C. D., Kitidis, V., Lapworth, D. J., Rees, A. P., Spears, B. M., Tye, A., Williamson, J. L., Balfour, C., Best, M., Bowes, M., Breimann, S., Brown, I. J., Burden, A., Callaghan, N., Felgate, S. L., Fishwick, J., Fraser, M., Gibb, S. W., Gilbert, P. J., Godsell, N., Gomez-Castillo, A. P., Hargreaves, G., Jones, O., Kennedy, P., Lichtschlag, A., Martin, A., May, R., Mawji, E., Mounteney, I., Nightingale, P. D., Olszewska, J. P., Painter, S. C., Pearce, C. R., Pereira, M. G., Peel, K., Pickard, A., Stephens, J. A., Stinchcombe, M., Williams, P., Woodward, E. M. S., Yarrow, D., and Mayor, D. J.: Contrasting Estuarine Processing of Dissolved Organic Matter Derived From Natural and

- Human-Impacted Landscapes, Global Biogeochemical Cycles, 35, e2021GB007023, <https://doi.org/10.1029/2021GB007023>, 2021.
- Garvine, R., and Whitney, M.: An estuarine box model of freshwater delivery to the coastal ocean for use in climate models, *Journal of Marine Research*, 64, 173-194, 10.1357/002224006777606506, 2006.
- Gattuso, J. P., Frankignoulle, M., and Wollast, R.: Carbon and carbonate metabolism in coastal aquatic ecosystems, *Annual Review of Ecology and Systematics*, 29, 405-434, 10.1146/annurev.ecolsys.29.1.405, 1998.
- Geerts, L., Maris, T., and Meire, P.: An interestuarine comparison for ecology in TIDE - The Scheldt, Elbe, Humber and Weser, *Ecosystem Management Research Group*, Antwerp, Belgium, 89, 2013.
- Geerts, L., Cox, T. J. S., Maris, T., Wolfstein, K., Meire, P., and Soetaert, K.: Substrate origin and morphology differentially determine oxygen dynamics in two major European estuaries, the Elbe and the Schelde, *Estuarine, Coastal and Shelf Science*, 191, 157-170, <https://doi.org/10.1016/j.ecss.2017.04.009>, 2017.
- Hartman, S. E., Humphreys, M. P., Kivimäe, C., Woodward, E. M. S., Kitidis, V., McGrath, T., Hydes, D. J., Greenwood, N., Hull, T., Ostle, C., Pearce, D. J., Sivyer, D., Stewart, B. M., Walsham, P., Painter, S. C., McGovern, E., Harris, C., Griffiths, A., Smilenova, A., Clarke, J., Davis, C., Sanders, R., and Nightingale, P.: Seasonality and spatial heterogeneity of the surface ocean carbonate system in the northwest European continental shelf, *Progress in Oceanography*, 177, 101909, 10.1016/j.pocean.2018.02.005, 2019.
- Hartmann, J.: Bicarbonate-fluxes and CO<sub>2</sub>-consumption by chemical weathering on the Japanese Archipelago — Application of a multi-lithological model framework, *Chemical Geology*, 265, 237-271, <https://doi.org/10.1016/j.chemgeo.2009.03.024>, 2009.
- Hersbach, H., Bell, B., Berrisford, P., Biavati, G., Horányi, A., Muñoz Sabater, J., Nicolas, J., Peubey, C., Radu, R., Rozum, I., Schepers, D., Simmons, A., Soci, C., Dee, D., and Thépaut, J.-N.: ERA5 hourly data on pressure levels from 1979 to present. Copernicus Climate Change Service Climate Data Store (Ed.), 2018.
- Hudon, C., Gagnon, P., Rondeau, M., Hébert, S., Gilbert, D., Hill, B., Patoine, M., and Starr, M.: Hydrological and biological processes modulate carbon, nitrogen and phosphorus flux from the St. Lawrence River to its estuary (Quebec, Canada), *Biogeochemistry*, 135, 251-276, 10.1007/s10533-017-0371-4, 2017.
- Humphreys, M. P., Achterberg, E. P., Hopkins, J. E., Chowdhury, M. Z. H., Griffiths, A. M., Hartman, S. E., Hull, T., Smilenova, A., Wihsgott, J. U., S. Woodward, E. M., and Moore, M. C.: Mechanisms for a nutrient-conserving carbon pump in a seasonally stratified, temperate continental shelf sea, *Progress in Oceanography*, 10.1016/j.pocean.2018.05.001, 2018.
- Iriarte, A., and Purdie, D. A.: Distribution of chroococcoid cyanobacteria and size-fractionated chlorophyll a biomass in the central and southern north sea waters during June/July 1989, *Netherlands Journal of Sea Research*, 31, 53-56, [https://doi.org/10.1016/0077-7579\(93\)90016-L](https://doi.org/10.1016/0077-7579(93)90016-L), 1993.
- Jakobsen, H. H., and Markager, S.: Carbon-to-chlorophyll ratio for phytoplankton in temperate coastal waters: Seasonal patterns and relationship to nutrients, *Limnology and Oceanography*, 61, 1853-1868, <https://doi.org/10.1002/lno.10338>, 2016.
- Jarvie, H. P., Neal, C., Leach, D. V., Ryland, G. P., House, W. A., and Robson, A. J.: Major ion concentrations and the inorganic carbon chemistry of the Humber rivers, *Science of The Total Environment*, 194-195, 285-302, 10.1016/S0048-9697(96)05371-5, 1997a.
- Jarvie, H. P., Neal, C., and Robson, A. J.: The geography of the Humber catchment, *Science of The Total Environment*, 194-195, 87-99, [https://doi.org/10.1016/S0048-9697\(96\)05355-7](https://doi.org/10.1016/S0048-9697(96)05355-7), 1997b.
- Jarvie, H. P., King, S. M., and Neal, C.: Inorganic carbon dominates total dissolved carbon concentrations and fluxes in British rivers: Application of the THINCARB model – Thermodynamic modelling of inorganic carbon in freshwaters, *Science of The Total Environment*, 575, 496-512, <https://doi.org/10.1016/j.scitotenv.2016.08.201>, 2017.
- Jiang, Z.-P., Yuan, J., Hartman, S. E., and Fan, W.: Enhancing the observing capacity for the surface ocean by the use of Volunteer Observing Ship, *Acta Oceanologica Sinica*, 38, 114-120, 10.1007/s13131-019-1463-3, 2019.
- Jickells, T., Andrews, J., Samways, G., Sanders, R., Malcolm, S., Sivyer, D., Parker, R., Nedwell, D., Trimmer, M., and Ridgway, J.: Nutrient Fluxes through the Humber Estuary: Past, Present and Future, *Ambio*, 29, 130-135, 2000.
- Joesoef, A., Kirchman, D. L., Sommerfield, C. K., and Cai, W. J.: Seasonal variability of the inorganic carbon system in a large coastal plain estuary, *Biogeosciences*, 14, 4949-4963, 10.5194/bg-14-4949-2017, 2017.

- 815 Juhls, B., Overduin, P. P., Hölemann, J., Hieronymi, M., Matsuoka, A., Heim, B., and Fischer, J.: Dissolved organic matter at the fluvial–marine transition in the Laptev Sea using in situ data and ocean colour remote sensing, *Biogeosciences*, 16, 2693-2713, 10.5194/bg-16-2693-2019, 2019.
- Kerimoglu, O., Große, F., Kreuz, M., Lenhart, H.-J., and van Beusekom, J. E. E.: A model-based projection of historical state of a coastal ecosystem: Relevance of phytoplankton stoichiometry, *Science of The Total Environment*, 639, 1311-1323, 10.1016/j.scitotenv.2018.05.215, 2018.
- 820 Kerimoglu, O., Voynova, Y. G., Chegini, F., Brix, H., Callies, U., Hofmeister, R., Klingbeil, K., Schrum, C., and van Beusekom, J. E. E.: Interactive impacts of meteorological and hydrological conditions on the physical and biogeochemical structure of a coastal system, *Biogeosciences*, 17, 5097-5127, 10.5194/bg-17-5097-2020, 2020.
- Kerner, M.: Effects of deepening the Elbe Estuary on sediment regime and water quality, *Estuarine, Coastal and Shelf Science*, 75, 492-500, <https://doi.org/10.1016/j.ecss.2007.05.033>, 2007.
- 825 Kitidis, V., Shutler, J. D., Ashton, I., Warren, M., Brown, I., Findlay, H., Hartman, S. E., Sanders, R., Humphreys, M., Kivimäe, C., Greenwood, N., Hull, T., Pearce, D., McGrath, T., Stewart, B. M., Walsham, P., McGovern, E., Bozec, Y., Gac, J.-P., van Heuven, S. M. A. C., Hoppema, M., Schuster, U., Johannessen, T., Omar, A., Lauvset, S. K., Skjelvan, I., Olsen, A., Steinhoff, T., Körtzinger, A., Becker, M., Lefevre, N., Diverres, D., Gkritzalis, T., Cattrijsse, A., Petersen, W.,
- 830 Voynova, Y. G., Chapron, B., Grouazel, A., Land, P. E., Sharples, J., and Nightingale, P. D.: Winter weather controls net influx of atmospheric CO<sub>2</sub> on the north-west European shelf, *Scientific Reports*, 9, 20153, 10.1038/s41598-019-56363-5, 2019.
- Kühn, W., Pätsch, J., Thomas, H., Borges, A. V., Schiettecatte, L.-S., Bozec, Y., and Prowe, A. E. F.: Nitrogen and carbon cycling in the North Sea and exchange with the North Atlantic—A model study, Part II: Carbon budget and fluxes, *Continental Shelf Research*, 30, 1701-1716, 10.1016/j.csr.2010.07.001, 2010.
- 835 Kuliński, K., Pempkowiak, J., and Herndl, G.: The carbon budget of the Baltic Sea, *Biogeosciences*, 8, 2011.
- Kvale, E. P.: The origin of neap–spring tidal cycles, *Marine Geology*, 235, 5-18, <https://doi.org/10.1016/j.margeo.2006.10.001>, 2006.
- Lacroix, F., Ilyina, T., Mathis, M., Laruelle, G. G., and Regnier, P.: Historical increases in land-derived nutrient inputs may alleviate effects of a changing physical climate on the oceanic carbon cycle, *Global Change Biology*, 27, 5491-5513, <https://doi.org/10.1111/gcb.15822>, 2021.
- 840 Laruelle, G. G., Dürr, H. H., Slomp, C. P., and Borges, A. V.: Evaluation of sinks and sources of CO<sub>2</sub> in the global coastal ocean using a spatially-explicit typology of estuaries and continental shelves, *Geophysical Research Letters*, 37, 10.1029/2010GL043691, 2010.
- 845 Legge, O., Johnson, M., Hicks, N., Jickells, T., Diesing, M., Aldridge, J., Andrews, J., Artioli, Y., Bakker, D. C. E., Burrows, M. T., Carr, N., Cripps, G., Felgate, S. L., Fernand, L., Greenwood, N., Hartman, S., Kröger, S., Lessin, G., Mahaffey, C., Mayor, D. J., Parker, R., Queirós, A. M., Shutler, J. D., Silva, T., Stahl, H., Tinker, J., Underwood, G. J. C., Van Der Molen, J., Wakelin, S., Weston, K., and Williamson, P.: Carbon on the Northwest European Shelf: Contemporary Budget and Future Influences, *Frontiers in Marine Science*, 7, 143, 2020.
- 850 Lehmann, N., Stacke, T., Lehmann, S., Lantuit, H., Gosse, J., Mears, C., Hartmann, J., and Thomas, H.: Alkalinity responses to climate warming destabilise the Earth’s thermostat, *Nature Communications*, 14, 1648, 10.1038/s41467-023-37165-w, 2023.
- Lorkowski, I., Pätsch, J., Moll, A., and Kühn, W.: Interannual variability of carbon fluxes in the North Sea from 1970 to 2006 – Competing effects of abiotic and biotic drivers on the gas-exchange of CO<sub>2</sub>, *Estuarine, Coastal and Shelf Science*, 100, 38-57, 10.1016/j.ecss.2011.11.037, 2012.
- 855 Lucas, A. J., Franks, P. J. S., and Dupont, C. L.: Horizontal internal-tide fluxes support elevated phytoplankton productivity over the inner continental shelf, *Limnology and Oceanography: Fluids and Environments*, 1, 56-74, <https://doi.org/10.1215/21573698-1258185>, 2011.
- Lucas, L. V., Koseff, J. R., Monismith, S. G., Cloern, J. E., and Thompson, J. K.: Processes governing phytoplankton blooms in estuaries. II: The role of horizontal transport, *Marine Ecology Progress Series*, 187, 17-30, 1999.
- 860 Macintyre, H., and Cullen, J.: Primary production by suspended and benthic microalgae in a turbid estuary: Time-scales of variability in San Antonio Bay, Texas, *Marine Ecology Progress Series*, 145, 245-268, 10.3354/meps145245, 1996.

- Macovei, V. A., Petersen, W., Brix, H., and Voynova, Y. G.: Reduced Ocean Carbon Sink in the South and Central North Sea (2014–2018) Revealed From FerryBox Observations, *Geophysical Research Letters*, 48, e2021GL092645, 10.1029/2021GL092645, 2021a.
- Macovei, V. A., Voynova, Y. G., Becker, M., Triest, J., and Petersen, W.: Long-term intercomparison of two pCO<sub>2</sub> instruments based on ship-of-opportunity measurements in a dynamic shelf sea environment, *Limnology and Oceanography: Methods*, 19, 37–50, 10.1002/lom3.10403, 2021b.
- Macovei, V. A., Voynova, Y. G., Gehrung, M., and Petersen, W.: Ship-of-Opportunity, FerryBox-integrated, membrane-based sensor pCO<sub>2</sub>, temperature and salinity measurements in the surface North Sea since 2013. PANGAEA, 2021c.
- Macovei, V. A., Callies, U., Calil, P. H. R., and Voynova, Y. G.: Mesoscale Advective and Biological Processes Alter Carbon Uptake Capacity in a Shelf Sea, *Frontiers in Marine Science*, 9, 2022.
- McDougall, T. J., and Barker, P. M.: Getting started with TEOS-10 and the Gibbs Seawater (GSW) Oceanographic Toolbox., SCOR/IAPSO WG127, 2011.
- McKenna, J. H.: DOC dynamics in a small temperate estuary: Simultaneous addition and removal processes and implications on observed nonconservative behavior, *Estuaries*, 27, 604–616, 10.1007/BF02907648, 2004.
- Murrell, M. C., and Lores, E. M.: Phytoplankton and zooplankton seasonal dynamics in a subtropical estuary: importance of cyanobacteria, *Journal of Plankton Research*, 26, 371–382, 10.1093/plankt/fbh038, 2004.
- Newton, R. M., Weintraub, J., and April, R.: The Relationship between Surface Water Chemistry and Geology in the North Branch of the Moose River, *Biogeochemistry*, 3, 21–35, 1987.
- Orr, J. C., Epitalon, J.-M., Dickson, A. G., and Gattuso, J.-P.: Routine uncertainty propagation for the marine carbon dioxide system, *Marine Chemistry*, 207, 84–107, <https://doi.org/10.1016/j.marchem.2018.10.006>, 2018.
- Osterholz, H., Burmeister, C., Busch, S., Dierken, M., Frazão, H. C., Hansen, R., Jeschek, J., Kremp, A., Kreuzer, L., Sadkowiak, B., Waniek, J. J., and Schulz-Bull, D. E.: Nearshore Dissolved and Particulate Organic Matter Dynamics in the Southwestern Baltic Sea: Environmental Drivers and Time Series Analysis (2010–2020), *Frontiers in Marine Science*, 8, 2021.
- Painter, S. C., Lapworth, D. J., Woodward, E. M. S., Kroeger, S., Evans, C. D., Mayor, D. J., and Sanders, R. J.: Terrestrial dissolved organic matter distribution in the North Sea, *Science of The Total Environment*, 630, 630–647, <https://doi.org/10.1016/j.scitotenv.2018.02.237>, 2018.
- Petersen, W.: FerryBox systems: State-of-the-art in Europe and future development, *Journal of Marine Systems*, 140, 4–12, 10.1016/j.jmarsys.2014.07.003, 2014.
- Petersen, W., and Colijn, F.: FerryBox white paper, EUROGOOS PUBLICATION 2017 [http://eurogoos.eu/download/publications/EuroGOOS\\_Ferrybox\\_whitepaper\\_2017.pdf](http://eurogoos.eu/download/publications/EuroGOOS_Ferrybox_whitepaper_2017.pdf), 2017.
- Prowe, A. E. F., Thomas, H., Pätsch, J., Kühn, W., Bozec, Y., Schiettecatte, L.-S., Borges, A. V., and de Baar, H. J. W.: Mechanisms controlling the air–sea CO<sub>2</sub> flux in the North Sea, *Continental Shelf Research*, 29, 1801–1808, 10.1016/j.csr.2009.06.003, 2009.
- Pugach, S. P., Pipko, I. I., Shakhova, N. E., Shirshin, E. A., Perminova, I. V., Gustafsson, Ö., Bondur, V. G., Ruban, A. S., and Semiletov, I. P.: Dissolved organic matter and its optical characteristics in the Laptev and East Siberian seas: spatial distribution and interannual variability (2003–2011), *Ocean Sci.*, 14, 87–103, 10.5194/os-14-87-2018, 2018.
- Quiel, K., Becker, A., Kirchesch, V., Schöl, A., and Fischer, H.: Influence of global change on phytoplankton and nutrient cycling in the Elbe River, *Regional Environmental Change*, 11, 405–421, 10.1007/s10113-010-0152-2, 2011.
- Raymond, P. A., Bauer, J. E., and Cole, J. J.: Atmospheric CO<sub>2</sub> evasion, dissolved inorganic carbon production, and net heterotrophy in the York River estuary, *Limnology and Oceanography*, 45, 1707–1717, <https://doi.org/10.4319/lo.2000.45.8.1707>, 2000.
- Regnier, P., Arndt, S., Goossens, N., Volta, C., Laruelle, G. G., Lauerwald, R., and Hartmann, J.: Modelling Estuarine Biogeochemical Dynamics: From the Local to the Global Scale, *Aquatic Geochemistry*, 19, 591–626, 10.1007/s10498-013-9218-3, 2013.
- Regnier, P., Resplandy, L., Najjar, R. G., and Ciais, P.: The land-to-ocean loops of the global carbon cycle, *Nature*, 603, 401–410, 10.1038/s41586-021-04339-9, 2022.
- Reimer, A., Brasse, S., Doerffer, R., Dürselen, C. D., Kempe, S., Michaelis, W., Rick, H. J., and Seifert, R.: Carbon cycling in the German Bight: An estimate of transformation processes and transport, *Deutsche Hydrografische Zeitschrift*, 51, 313–329, 10.1007/BF02764179, 1999.



- Reimer, J. J., Wang, H., Vargas, R., and Cai, W.-J.: Multidecadal fCO<sub>2</sub> Increase Along the United States Southeast Coastal Margin, *Journal of Geophysical Research: Oceans*, 122, 10061-10072, <https://doi.org/10.1002/2017JC013170>, 2017.
- 915 Rewrie, L. C. V., Baschek, B., Beusekom, J. E. E., Körtzinger, A., Ollesch, G., and Voynova, Y. G.: Recent inorganic carbon increase in a temperate estuary driven by water quality improvement and enhanced by droughts, *EGU sphere*, 2023, 1-28, 10.5194/egusphere-2023-961, 2023a.
- Rewrie, L. C. V., Voynova, Y. G., van Beusekom, J. E. E., Sanders, T., Körtzinger, A., Brix, H., Ollesch, G., and Baschek, B.: Significant shifts in inorganic carbon and ecosystem state in a temperate estuary (1985–2018), *Limnology and Oceanography*, n/a, <https://doi.org/10.1002/lno.12395>, 2023b.
- 920 Rewrie, L. C. V., Baschek, B., Van Beusekom, J. E. E., Kortzinger, A., Petersen, W., Rottgers, R., and Voynova, Y. G.: Impact of primary production and net ecosystem metabolism on carbon and nutrient cycling at the land-sea interface, *Frontiers in Marine Science*, 12, 10.3389/fmars.2025.1548463, 2025.
- Riemann, B., Carstensen, J., Dahl, K., Fossing, H., Hansen, J. W., Jakobsen, H. H., Josefson, A. B., Krause-Jensen, D., Markager, S., Stæhr, P. A., Timmermann, K., Windolf, J., and Andersen, J. H.: Recovery of Danish Coastal Ecosystems After Reductions in Nutrient Loading: A Holistic Ecosystem Approach, *Estuaries and Coasts*, 39, 82-97, 10.1007/s12237-015-9980-0, 2016.
- 925 Rocha, C., Galvão, H. M., and Barbosa, A.: Role of transient silicon limitation in the development of cyanobacteria blooms in the Guadiana estuary, south-western Iberia, *Marine Ecology Progress Series*, 228, 35-45, 2002.
- 930 Sanders, R. J., Jickells, T., Malcolm, S., Brown, J., Kirkwood, D., Reeve, A., Taylor, J., Horrobin, T., and Ashcroft, C.: Nutrient fluxes through the Humber estuary, *Journal of Sea Research*, 37, 3-23, [https://doi.org/10.1016/S1385-1101\(96\)00002-0](https://doi.org/10.1016/S1385-1101(96)00002-0), 1997.
- Schiettecatte, L. S., Thomas, H., Bozec, Y., and Borges, A. V.: High temporal coverage of carbon dioxide measurements in the Southern Bight of the North Sea, *Marine Chemistry*, 106, 161-173, 10.1016/j.marchem.2007.01.001, 2007.
- 935 Schlarbaum, T., Daehnke, K., and Emeis, K.: Turnover of combined dissolved organic nitrogen and ammonium in the Elbe estuary/NW Europe: Results of nitrogen isotope investigations, *Marine Chemistry*, 119, 91-107, <https://doi.org/10.1016/j.marchem.2009.12.007>, 2010.
- Sharples, J., Tweddle, J. F., Mattias Green, J. A., Palmer, M. R., Kim, Y.-N., Hickman, A. E., Holligan, P. M., Moore, C. M., Rippeth, T. P., Simpson, J. H., and Krivtsov, V.: Spring-neap modulation of internal tide mixing and vertical nitrate fluxes at a shelf edge in summer, *Limnology and Oceanography*, 52, 1735-1747, <https://doi.org/10.4319/lo.2007.52.5.1735>, 2007.
- 940 Shen, C., Testa, J. M., Ni, W., Cai, W.-J., Li, M., and Kemp, W. M.: Ecosystem Metabolism and Carbon Balance in Chesapeake Bay: A 30-Year Analysis Using a Coupled Hydrodynamic-Biogeochemical Model, *Journal of Geophysical Research: Oceans*, 124, 6141-6153, <https://doi.org/10.1029/2019JC015296>, 2019.
- 945 Smith, S. V., and Hollibaugh, J. T.: Coastal metabolism and the oceanic organic carbon balance, *Reviews of Geophysics*, 31, 75-89, <https://doi.org/10.1029/92RG02584>, 1993.
- Thomas, H., Bozec, Y., de Baar, H. J. W., Elkalay, K., Frankignoulle, M., Schiettecatte, L. S., Kattner, G., and Borges, A. V.: The carbon budget of the North Sea, *Biogeosciences*, 2, 87-96, 10.5194/bg-2-87-2005, 2005.
- Tipping, E., Marker, A. F. H., Butterwick, C., Collett, G. D., Cranwell, P. A., Ingram, J. K. G., Leach, D. V., Lishman, J. P., Pinder, A. C., Rigg, E., and Simon, B. M.: Organic carbon in the Humber rivers, *Science of The Total Environment*, 194-195, 345-355, [https://doi.org/10.1016/S0048-9697\(96\)05374-0](https://doi.org/10.1016/S0048-9697(96)05374-0), 1997.
- 950 Trigueros, J. M., and Orive, E.: Tidally driven distribution of phytoplankton blooms in a shallow, macrotidal estuary, *Journal of Plankton Research*, 22, 969-986, 10.1093/plankt/22.5.969, 2000.
- Tsunogai, S., Watanabe, S., and Sato, T.: Is there a "continental shelf pump" for the absorption of atmospheric CO<sub>2</sub>?, *Tellus Series B-Chemical and Physical Meteorology*, 51, 701-712, 10.1034/j.1600-0889.1999.t01-2-00010.x, 1999.
- 955 Turnewitsch, R., Dale, A., Lahajnar, N., Lampitt, R. S., and Sakamoto, K.: Can neap-spring tidal cycles modulate biogeochemical fluxes in the abyssal near-seafloor water column?, *Progress in Oceanography*, 154, 1-24, <https://doi.org/10.1016/j.pocean.2017.04.006>, 2017.
- van Heuven, S., Pierrot, D., Rae, J. W. B., Lewis, E., and Wallace, D. W. R.: CO<sub>2</sub>SYST v 1.1 MATLAB Program Developed for CO<sub>2</sub> System Calculations. ORNL/CDIAC-105b. In: MATLAB Program Developed for CO<sub>2</sub> System Calculations. ORNL/CDIAC-105b., Oak Ridge National Laboratory, Oak Ridge, Tennessee, 2011.
- 960

- Volta, C., Laruelle, G. G., and Regnier, P.: Regional carbon and CO<sub>2</sub> budgets of North Sea tidal estuaries, *Estuarine, Coastal and Shelf Science*, 176, 76-90, 10.1016/j.ecss.2016.04.007, 2016.
- 965 Voynova, Y. G., Lebaron, K. C., Barnes, R. T., and Ullman, W. J.: In situ response of bay productivity to nutrient loading from a small tributary: The Delaware Bay-Murderkill Estuary tidally-coupled biogeochemical reactor, *Estuarine, Coastal and Shelf Science*, 160, 33-48, <https://doi.org/10.1016/j.ecss.2015.03.027>, 2015.
- Voynova, Y. G., Brix, H., Petersen, W., Sieglind, W.-K., and Scharfe, M.: Extreme flood impact on estuarine and coastal biogeochemistry: The 2013 Elbe flood, *Biogeosciences*, 14, 541-557, 10.5194/bg-14-541-2017, 2017.
- 970 Voynova, Y. G., Petersen, W., Gehrung, M., Aßmann, S., and King, A. L.: Intertidal regions changing coastal alkalinity: The Wadden Sea-North Sea tidally coupled bioreactor, *Limnology and Oceanography*, 64, 1135-1149, 10.1002/lno.11103, 2019.
- Wanninkhof, R.: Relationship between wind speed and gas exchange over the ocean revisited, *Limnology and Oceanography-Methods*, 12, 351-362, 10.4319/lom.2014.12.351, 2014.
- Ward, N. D., Bianchi, T. S., Medeiros, P. M., Seidel, M., Richey, J. E., Keil, R. G., and Sawakuchi, H. O.: Where Carbon Goes When Water Flows: Carbon Cycling across the Aquatic Continuum, *Frontiers in Marine Science*, 4, 2017.
- 975 Webb, K. L., and D'Elia, C. F.: Nutrient and Oxygen Redistribution During a Spring Neap Tidal Cycle in a Temperate Estuary, *Science*, 207, 983-985, 10.1126/science.207.4434.983, 1980.
- Weiss, R. F.: Carbon dioxide in water and seawater: the solubility of a non-ideal gas, *Marine Chemistry*, 2, 203-215, [https://doi.org/10.1016/0304-4203\(74\)90015-2](https://doi.org/10.1016/0304-4203(74)90015-2), 1974.
- Weston, K., Jickells, T. D., Fernand, L., and Parker, E. R.: Nitrogen cycling in the southern North Sea: consequences for total nitrogen transport, *Estuarine, Coastal and Shelf Science*, 59, 559-573, 10.1016/j.ecss.2003.11.002, 2004.
- 980 Williamson, J. L., Tye, A., Lapworth, D. J., Monteith, D., Sanders, R., Mayor, D. J., Barry, C., Bowes, M., Bowes, M., Burden, A., Callaghan, N., Farr, G., Felgate, S., Fitch, A., Gibb, S., Gilbert, P., Hargreaves, G., Keenan, P., Kitidis, V., Juergens, M., Martin, A., Mounteney, I., Nightingale, P. D., Pereira, M. G., Olszewska, J., Pickard, A., Rees, A. P., Spears, B., Stinchcombe, M., White, D., Williams, P., Worrall, F., and Evans, C.: Landscape controls on riverine export of dissolved organic carbon from Great Britain, *Biogeochemistry*, 164, 163-184, 10.1007/s10533-021-00762-2, 2023.
- 985 Wiltshire, K. H., Harsdorf, S., Smidt, B., Blöcker, G., Reuter, R., and Schroeder, F.: The determination of algal biomass (as chlorophyll) in suspended matter from the Elbe estuary and the German Bight: A comparison of high-performance liquid chromatography, delayed fluorescence and prompt fluorescence methods, *Journal of Experimental Marine Biology and Ecology*, 222, 113-131, [https://doi.org/10.1016/S0022-0981\(97\)00141-X](https://doi.org/10.1016/S0022-0981(97)00141-X), 1998.
- 990 World Data Centre for Greenhouse Gases: Mace Head xCO<sub>2</sub> <https://gaw.kishou.go.jp/>. 2020.
- Xing, Q., Yu, H., Yu, H., Wang, H., Ito, S.-i., and Yuan, C.: Evaluating the Spring-Neap Tidal Effects on Chlorophyll-a Variations Based on the Geostationary Satellite, *Frontiers in Marine Science*, 8, 2021.
- Yang, W., Wang, F., Liu, L.-N., and Sui, N.: Responses of Membranes and the Photosynthetic Apparatus to Salt Stress in Cyanobacteria, *Frontiers in Plant Science*, 11, 2020.
- 995 Zhai, W. D., Dai, M., and Cai, W. J.: Coupling of surface pCO<sub>2</sub> and dissolved oxygen in the northern South China Sea: impacts of contrasting coastal processes, *Biogeosciences*, 6, 2589-2598, 10.5194/bg-6-2589-2009, 2009.